

*AUS DEM LEHRSTUHL  
FÜR INNERE MEDIZIN I  
PROF. DR. MARTINA MÜLLER-SCHILLING  
DER FAKULTÄT FÜR MEDIZIN  
DER UNIVERSITÄT REGENSBURG*

***EFFECT OF BACTERIA-DERIVED INDOLE-3-PROPIONIC ACID (IPA) IN  
MURINE PRIMARY HEPATOCYTES***

Inaugural – Dissertation  
zur Erlangung des Doktorgrades  
*der Medizin*

der  
Fakultät für Medizin  
der Universität Regensburg

vorgelegt von  
*Max Wißmüller*

2016

Dekan: *Prof. Dr. Dr. Torsten E. Reichert*

1. Berichterstatter: *Prof. Dr. Claus Hellerbrand*

2. Berichterstatter: *Prof. Dr. Jonathan Jantsch*

Tag der mündlichen Prüfung: 29.06.2017

## Table of Contents

<b>1</b>	<b>Zusammenfassung</b>	<b>3</b>
<b>2</b>	<b>Introduction</b>	<b>5</b>
<b>3</b>	<b>Material and Methods</b>	<b>8</b>
<b>3.1</b>	<b>Microscopy</b>	<b>8</b>
3.1.1	Trypan Blue	8
3.1.2	Fluorescent dyes	8
<b>3.2</b>	<b>Cell isolation</b>	<b>9</b>
3.2.1	Animals	10
3.2.2	Procedure	10
3.2.3	Quality control: viability	14
<b>3.3</b>	<b>Primary cell culture</b>	<b>15</b>
<b>3.4</b>	<b>Cytotoxicity model</b>	<b>15</b>
3.4.1	Indole-3-propionic acid (IPA)	16
3.4.2	Carbon tetrachloride (CCl <sub>4</sub> )	17
3.4.3	Enzyme leakage	20
3.4.4	Oxidative stress	25
<b>3.5</b>	<b>Western Blot</b>	<b>27</b>
3.5.1	Homogenization of protein extracts	27
3.5.2	Protein concentration	28
3.5.3	Gel production	28
3.5.4	Electrophoresis	30
3.5.5	Blotting	31
3.5.6	Immunostaining	31
3.5.7	Densitometry	32
<b>3.6</b>	<b>Statistical Analysis</b>	<b>32</b>
3.6.1	Image analysis	33
3.6.2	Statistical analysis	33
<b>4</b>	<b>Results</b>	<b>33</b>
<b>4.1</b>	<b>Impact of IPA on primary hepatocyte cultures</b>	<b>34</b>
<b>4.2</b>	<b>Cytotoxicity model</b>	<b>34</b>
<b>4.3</b>	<b>Hepatoprotective effect of IPA</b>	<b>37</b>
4.3.1	First impression by dye uptake	37
4.3.2	CYP2E1 levels	38
4.3.3	Cell damage marker levels <i>in vitro</i>	39
4.3.4	Oxidative Stress in primary hepatocytes <i>in vitro</i>	44
<b>4.4</b>	<b>Role of IPA in hepatic metabolism in addition to antioxidant properties</b>	<b>46</b>
4.4.1	SOD1	46
4.4.2	HSP27	48
<b>5</b>	<b>Discussion</b>	<b>50</b>
<b>6</b>	<b>Bibliography</b>	<b>57</b>
<b>7</b>	<b>Acknowledgements</b>	<b>64</b>
<b>8</b>	<b>Curriculum Vitae</b>	<b>65</b>

## 1 Zusammenfassung

Die Leber des Menschen ist ein Organ mit erstaunlichen Selbstheilungskräften. Die Frage nach Faktoren, welche die Gesundheit und das Regenerationspotential dieses Organs erhalten ist seit langem Gegenstand wissenschaftlichen Interesses in der Hepatologie.

Anatomisch einzigartig erhält die Leber den Großteil ihrer Blutversorgung aus dem Darm. Es reiht sich ein vorgeschaltetes intestinales Kapillarstromgebiet an ein nachgeschaltetes hepatisches Kapillarstromgebiet. Mit Hilfe von Enterozyten werden Stoffe aus der Umwelt in den Blutkreislauf aufgenommen und gelangen über die Pfortader direkt und teils noch unverarbeitet in das hepatische Gewebe.

Diese im menschlichen Körper einzigartige Blutversorgung der Leber ist bereits anatomischer Ausdruck ihrer zentralen Funktion als Stoffwechselorgan des Menschen: zu ihren Aufgaben gehören zum Beispiel die Herstellung von Glucose, Cholesterin und körpereigenen Eiweißen; die Speicherung von Zuckern, Fetten und Vitaminen; die Beiteiligung an der Verdauung über die Produktion von Gallensäuren sowie der Abbau und die Entgiftung von Stoffwechselabfällen und zugeführten Stoffen wie Alkohol oder Medikamenten.

Unterstützt wird die Leber bei der Verstoffwechslung der Nahrung unter anderem von Bakterien im menschlichen Darm, welche entscheidend die Art und Zusammensetzung der aufgenommen und von der Leber weiterverarbeiteten Stoffe prägen. Die Rolle des in seiner Komplexität noch relativ unverstandenen Microbioms erscheint als ein neuer Ansatzpunkt in der hepatologischen Forschung und um unser Verständnins des Zusammenspiels von Leber und Darm zu erforschen, wurden in den letzten Jahrzehnten immer mehr wissenschaftliche Arbeiten angefertigt- in dieser Reihe will sich diese Arbeit eingliedern.

*Clostridium sporogenes*, ein physiologisch in der Darmflora des Menschen vorkommender Bakterienstamm, wurde von Wikoff et al. als alleiniger Produzent des antioxidativen Stoffes Indole-3-propionic acid (IPA) entdeckt. Ohne den Ursprung von IPA zu kennen, konnte Chyan et al. bereits in primären Neuronen erfolgreich einen protektiven Effekt gegen oxidativen Stress nachweisen.

In dieser Arbeit soll nun auf den Effekt von IPA auf primäre Hepatozyten eingegangen werden und eine potentielle symbiotische Regulierung des hepatozytären Metabolismus durch einen bakteriellen Stoff erforscht werden.

Methodologisch wurde eine primäre, murine Hepatozytenkultur einem etablierten, auf Chlorkohlenwasserstoff basierenden Zellschädigungs-Schema unterzogen. Eine quantitative und qualitative Analyse der Zellschädigung und Protein Expression auf zellulärer Ebene sollte Aufschluss über den möglichen Einfluss von IPA auf die Leberzelle geben.

Eine vermutete protektive Eigenschaft von IPA in der Leberzelle im Sinne eines Schutzes vor intrazellulärem oxidativem Stress konnte indirekt mittels einer signifikanten Verminderung der intrazellulären Oxidierung von Fetten bestätigt werden.

Eine durch Chlorkohlenwasserstoff ausgelöste Nekrose bzw. Zellschädigung der Hepatozyten konnte durch IPA signifikant und Dosis-abhängig vermindert werden, was durch mikroskopische Evaluation und durch Markerenzyme nachgewiesen wurde.

Mittels Western Blot und densitometrischer Quantifikation kann auch eine potentielle Induktion von bestimmten Enzymen (HSP27 und SOD1) durch IPA vermutet werden.

In Bezug auf den Stand der Forschung konnte die protektive, dosis-abhängige Eigenschaft des bakteriellen IPA erstmalig in primären Hepatozyten nachgewiesen werden. Die Induktion der Proteine HSP27 und SOD1 konnte in

Bezug auf Erkenntnisse der Arbeitsgruppe um Sakurai et al. als ambivalent im Sinne einer oxidativen Stress reduzierenden aber potentiell cancerogenen Wirkung kategorisiert werden. Diese Eigenschaft scheint IPA aufgrund des unklaren Ausmaßes an Induktion der Enzyme jedoch nicht grundsätzlich als potentiell Heilmittel zu disqualifizieren und weitere Langzeituntersuchung sollten an die durchgeführte Versuchsreihe angeschlossen werden. Jedoch ist die vorläufige Einschätzung des sehr wirksamen Antioxidants IPA mittels weiteren Ergebnisse zur Kanzerogenität zu überprüfen.

## 2 Introduction

The liver is the largest gland in the human body, representing 2.5% of the absolute body weight. It provides a multitude of metabolic functions that are fundamental to sustaining physiological homeostasis.<sup>1</sup>

The liver parenchyma consists of numerous liver lobules that contain hepatocytes and nonparenchymal liver cells, including Kupffer cells (KC), sinusoidal endothelial cells (SEC) and hepatic stellate cells (HSC). The unique parenchymal architecture of the liver lobules is modelled by hepatocytes, and their central role in liver physiology is underlined by their involvement in most of the liver's many functions.<sup>2</sup>

Most of the liver's blood supply comes from the intestine through the portal vein. This unique blood supply configuration makes the liver a central junction for the interplay between mammalian and bacterial metabolism. When intestinal permeability increases, the translocation of bacterial-derived products to the liver via the portal vein occurs.<sup>3</sup> For example, intestinal dysbiosis and bacterial translocation (BT) are common in patients with advanced liver disease, and the

translocation of bacteria contributes to alcoholic liver disease (ALD), whereas bacterial decontamination improves alcoholic liver disease.<sup>4-6</sup>

Central to this pathophysiological and most probably lipopolysaccharide (LPS)-mediated impact is the signalling via pattern recognition receptors, precisely the toll-like receptor family (TLR), which recognize bacteria-derived products and activate innate immune response.<sup>7</sup>

Activated HSC and KC maintain hepatic injury in liver fibrosis, steatohepatitis, and insulin resistance<sup>8</sup> by secreting inflammatory mediators. The activation is triggered by the interplay of bacterial products and the TLRs.<sup>9</sup>

In contrast to the focus on BT and intestinal barrier failure contributing to hepatic diseases, a new paradigm of a liver-gut axis has been formulated. Intriguing questions about the symbiosis of the gut microbiome and the liver remain unanswered.<sup>10,11</sup>

In a study that compared the plasma of germ-free mice and the plasma of conventional mice, findings based on a broad mass spectroscopy metabolomics study (conducted by Wikoff et al.) suggest an unexpectedly large effect of the microbiota on mammalian blood metabolites.<sup>12</sup>

Recently, Mazagova et al. made the novel observation that the microbiome is necessary for liver homeostasis, and an absence of bacteria and their products lead to escalated fibrosis upon hepatotoxin-induced chronic liver injury.<sup>11</sup>

One mechanism of hepatic protection that may be involved appears to be a direct targeting by bacterial metabolites.

Some amino acids are described as bacterial metabolites. The production of the indole-containing, melatonin-like metabolite Indole-3-propionic acid (IPA) was

recently discovered to be completely dependent on the presence of *Clostridium sporogenes*.<sup>12-14</sup>

Subsequently, the greater susceptibility of hepatocytes in germ-free mice to cell death following TAA treatment (Mazagova et al.) was hypothesized as a consequence of the absence of bacterial-derived IPA.

Furthermore, bacterial-derived IPA has recently been found to serve as a ligand for the xenobiotic sensor pregnane X receptor (PXR). PXR-deficient mice show a distinctly leaky gut as well as an upregulation of the toll-like receptor signalling pathway. In vivo IPA downregulated enterocyte-mediated inflammatory cytokine and enterocyte tumor necrosis factor- $\alpha$  (TNF- $\alpha$ ). At the same time, it upregulated junctional protein-coding mRNAs in enterocytes.<sup>15,16</sup>

In line with this concept of symbiosis and the inherent idea of microbiome cross-talk to the gut and liver promoted by their close proximity, investigations of the biochemical details of the liver-gut axis were further encouraged by interdisciplinary results of neurologic research.

Emerging evidence suggests that intestinal homeostasis and the microbiome are playing a considerable role in neurological diseases. For instance, in amyotrophic lateral sclerosis (ALS), a decreased level of antimicrobial defensins, which are produced physiologically in Paneth cells and help shape the microbiome, seem to be involved in the disease progression.<sup>17</sup>

Reactive oxygen species (ROS) are central to the onset of a variety of chronic diseases such as Alzheimer`s, Parkinson`s, ALS, and other neurological diseases that are caused by increased ROS levels.<sup>18</sup>

Chyan et al. found the bacteria-derived indoleamine IPA, which has been detected in the cerebrospinal fluid of humans, to completely protect primary neurons from oxidative stress, such as that caused by the amyloid beta-protein in Alzheimer`s disease. Chyan et al. focused on the radical scavenging capacity of IPA, which was found to even surpass the antioxidant potential of melatonin.<sup>19</sup>



In reviewing the literature, data was found that IPA has not only neuroprotective properties but protective effects on hepatic microsomal membranes incubated with iron-induced oxidative stress.<sup>19,20</sup>

This study is designed to test the hypothesis of a protective effect of IPA on primary hepatocytes in vitro and wants to clarify the potential of IPA as new drug in hepatologic disorders. Derived from current research results a first proof of hepatoprotective effect shall be followed by investigations on the concept of hepatoprotective mechanisms of IPA.

### **3 Material and Methods**

#### **3.1 Microscopy**

All microscopy was performed with a combined light and fluorescent microscope (Olympus IX71 Microscope, USA). Images presented in this study were captured with this microscope.

##### **3.1.1 Trypan Blue**

The commonly used Trypan Blue dye exclusion test is based on the principle of viable cells excluding dyes such as Trypan Blue. Indeed, dead cells do become permeable for the dye and take it up. Trypan Blue Stain (0.4%, GIBCO) was used to calculate the viability of isolated primary hepatocytes in this study.

##### **3.1.2 Fluorescent dyes**

To evaluate the physiological status and to detect living, dead, and apoptotic cells, primary hepatocytes were stained with fluorescent dyes.

### 3.1.2.1 *Hoechst*

Cells were stained with the DNA-binding dye Hoechst 33258 (Invitrogen, Carlsbad, CA) after treatment with carbon tetrachloride (CCl<sub>4</sub>). Hallmarks of apoptosis, including nuclear condensation, chromatic margination, and fragmentation, were then appraised.<sup>21,22</sup>

### 3.1.2.2 *Propidium Iodide*

Degradation of internucleosomal DNA in apoptosis correlates with the intensity of staining with a DNA-adhering fluorescent dye such as Propidium Iodide (Propidium Iodide, Sigma, USA), which can be useful in quantifying DNA degradation and apoptosis in cells.<sup>23,24</sup>

## 3.2 Cell isolation

Today, isolation of hepatocytes is a basic method used in liver research<sup>25</sup> that enables investigators to evaluate liver function in vitro. Primary hepatocytes have proven to provide a significantly better replication of liver organ function compared to immortalized cell lines when cultured.<sup>26</sup>

The technique described in the following paragraph was developed by Berry and Friend in 1969<sup>27</sup> and has undergone many modifications.<sup>28,29</sup> In a surgical procedure, a liver as a whole organ is resected and hepatocytes are released. A two-step collagenase perfusion is performed, in which the physiological liver architecture is disbanded by enzymatic digestion. A non-recirculating perfusion through the portal vein was used in this study.

The hepatocytes were separated from the remaining cells by filtration and centrifugation. The success of the isolation procedure can be assessed by light-microscopy via dye-exclusion of viable cells.

### **3.2.1 Animals**

Male wild-type C57BL/6 mice were purchased from Charles River (Wilmington, MA, USA) and bred in a vivarium at the UCSD Biomedical Research Building (Leichtag-Building), in San Diego, in a specific pathogen-free (SPF) environment. All animals were nurtured with a standard diet and had drinking water ad libidum. The age of the animals used in the study ranged from at least 6 weeks to a few months.

### **3.2.2 Procedure**

The hepatocytes used in the study were obtained using the following procedure: (1) preparation of the perfusion liquids, operating room, and anaesthesia; (2) the mouse surgery is performed with intraoperative liver perfusion, removal of the liver, and harvesting of hepatocytes; and (3) quality control is conducted.

#### ***3.2.2.1 Preparation of two-step collagenase digestion***

Cell isolation is a delicate process that needs to be performed accurately to guarantee an optimal result. The perfusion buffers for the two-step collagenase digestion were stock preparations of SC1 and SC2.

All the chemicals listed in table 1 were weighed with an analytical balance (AB54-S, Mettler Toledo, Switzerland) and, along with  $\text{CaCl}_2 \times 2\text{H}_2\text{O}$  that was added just

before use, added to water to generate the final concentrations of the stock solutions.

To adjust both aqueous solutions to physiological pH-values to ensure the optimal acidity for the digesting enzymes, the pH was adjusted to 7.35 using an electronic pH meter (Accumed BASIC AB15, Fisher, USA).

Subsequently, both solutions were filtered in a sterile manner using a 0.22µm filter (Steritop, vacuumdriven, 0.22µm, Millipore, USA) and stored at room temperature until use.

Prior to commencing the procedure, the perfusion buffers SC1 and SC2 were stored in autoclaved bottles.

Regarding the time-dependent enzyme activity of the used collagenases and the vulnerability of hepatocytes, precautionary measures were taken as described in the following paragraph.

The bottles were kept in a 42°C water bath during the whole procedure to maintain an adequate temperature of 37°C when entering the organ after passing through the plastic tubing system.

The SC2 was already warmed in a water bath, and shortly before use, the digestion enzymes were put into solution and  $\text{CaCl}_2 \times 2\text{H}_2\text{O}$  was added at the concentration given in table 1. To confirm that an ample and standardized enzyme activity was occurring, the solution was used no later than 30 minutes after dissolving the collagenases. The enzymes used for digestion were Collagenase P (produced in *Clostridium histolyticum*, Roche, USA), which has an enzyme activity of 1.74 U/mg in a concentration of 50mg/l, and Collagenase D (produced in *Clostridium histolyticum*, Roche, USA) which has an enzyme activity of >15 U/mg in a concentration of 500 mg/l.

**Table 1:** Recipe of SC-1 and SC-2

	<u>SC-1</u>	<u>SC-2</u>
NaCl <sub>2</sub>	8000mg/l	8000mg/l
KCl	400mg/l	400mg/l
NaH <sub>2</sub> PO <sub>4</sub> .H <sub>2</sub> O	78mg/l	78mg/l
Na <sub>2</sub> HPO <sub>4</sub>	120.45mg/l	120.45mg/l
HEPES	2380mg/l	2380mg/l
NaHCO <sub>3</sub>	350mg/l	350mg/l
EGTA	190mg/l	(-)
Glucose	900mg/l	(-)
CaCl <sub>2</sub> × 2H <sub>2</sub> O	(-)	560mg/l (just before use)

### 3.2.2.2 *Liver perfusion in situ*

In order to extract vital hepatocytes, a two-step collagenase digestion was performed in situ. Retrograde perfusion of the liver first with SC1 followed by SC2 through a perfusion system entering the portal vein was conducted. The liver was removed as a whole organ and transferred to a sterile cell culture hood (SterilGardHood Class II, the Baker Company, USA).

Mice were anesthetized using an isotonic solution (BBL Saline, Normal, 10ml, BD, USA) containing 1% xylazine (AnaSed Injection, c=100mg/ml Xylazine-Hydrochlorid, LLOYD, USA) and 6% ketamin (KetaSet C3, c=100mg/ml Ketamin, Fort Dodge Animal Health, USA). After 0.4ml of anaesthetics were applied via intraperitoneal injection, consciousness was tested repeatedly.

The abdomen was prepared with 70% ethanol-solution in order to ensure sterilization of the operating area for the surgical procedure. With a midline incision of the abdominal skin, the abdominal cavity was opened. The portal vein was exposed by gently moving the viscera to the side with a sterile cotton bud. Next, a sterile 20-gage catheter (Safelet Cath, 20G x 1", EXEL, USA) was inserted in the inferior vena cava (IVC) and fixed with surgical string (0.7 metric, 45cm, Henry Schein, USA). The intravenous catheter was connected to the tubes of the perfusion system, which included a pump (Masterflex, Modell 7518-00, Cole Parmer Inc., USA), plastic tubes, and a 42°C water bath for the SC1 and SC2 solutions. A filter (25mm Syringe Filter, 0.2 µm, Fisherbrand, USA) was placed in between the catheter and the tubes.

Perfusion was started with SC1 with a flow rate of 10ml/min for 5 minutes. As soon as the liver macroscopically started to change color (caused by blood drainage, indicating a correct cannulation and adequate position of the catheter), the hepatic portal vein was cut to allow efflux and to prevent portal hypertension. Directly after efflux of the perfusion buffer via the portal vein was evident, a thoracotomy was performed and the diaphragm was cut to expose the superior vena cava (SVC), which was carefully blocked with surgical tweezers to allow more efficient perfusion of the liver.

Next, the perfusion was continued after switching to the SC2 solution. The liver became swollen and pale, indicating that the perfusion was carried out successfully. To estimate the degree of parenchymal digestion, touching the organ with a sterile cotton bud tested its turgor and provided a clue for determining the perfusion endpoint. Hepatectomy was carried out cautiously after 5 to 8 minutes of perfusion with SC2 when digestion was completed. Finally, the liver was transferred to a sterile 100mm Petri dish containing 30ml of SC2 at 4°C, and subsequent work was performed under the cell culture hood.

### 3.2.2.3 *Isolation of Hepatocytes*

Liver cells were further processed in a gentle manner, taking their vulnerability into consideration. Vital hepatocytes for cell culture were purified by washing, filtration, and centrifugation.

Once placed in the Petri dish, the capsule of the extracted liver was opened with sterile forceps, and cells were allowed to disperse into the SC2 at 4°C. Cell dispersion was filtered through a 70µm pore-size cell strainer (Nylon Cell Strainer, BD Falcon, USA) into a 50ml conical tube. Connective tissue and undigested tissue fragments remained in the filter, and cells were resuspended in 40ml of SC2 at 4°C. To separate the vital from dead cells, centrifugation (Allegra 6R Centrifuge, Beckmann Coulter, USA) was performed twice at 450rpm for 1 minute at 4 °C. After the first centrifugation, the supernatant was carefully removed by vacuum and cells were gently resuspended by washing with media (Media 199 without Phenolred, Gibco, USA). Finally, the hepatocytes were resuspended a second time with 25ml of media containing 10% Fetal Calf Serum (FCS, Sigma-Aldrich, USA) at 37 °C.

### 3.2.3 **Quality control: viability**

Viability was one of the main criteria for quality control of the isolated cells. Trypan Blue Stain 0.4% (GIBCO, USA) was used to distinguish dead cells as described in section 3.1.1.

Due to loss of cell membrane integrity of dead hepatocytes, Trypan Blue stained them. Each 10µl of primary hepatocyte suspension and Trypan Blue were mixed (directly after the isolation) and counted in a counting chamber (Bright-Line Hemacytometer SET, Hausser Scientific, USA) using light microscopy. Total viability (V) was calculated by ratio of vital cells (vc) to total cells counted(tc) ( $V = vc/tc \times 100$ ).

### 3.3 Primary cell culture

The hepatocytes were plated, and cellshape and confluency were monitored microscopically. An adequate environment for primary hepatocytes was confirmed, and the medium was adapted as needed for the experimental setting.<sup>30</sup>

Cells were plated in 6-well Multiwell Plates (Tissue-culture treated polystyrene, flat bottom, low-evaporation lid, BD Falcon, USA) pre-coated with collagen. In order to pre-coat each well, a solution containing 30% ethanol and rat collagen type 1 (Collagen Type 1, Rat Tail, BD Biosciences, USA) was produced. Subsequently, in total 22.18 µg of collagen per well were dispensed within the solution and the solution was distributed equally in each well (by placing the plates on a shaker at high speed). Afterwards, plates were stored under the hood and air dried with the lid open for at least 30 minutes to facilitate the complete evaporation of the alcoholic components.

The total number of cells collected during isolation was calculated using a cell counting chamber. These values typically ranged from  $20 \times 10^6$  to  $30 \times 10^6$ . In each well,  $9 \times 10^5$  primary hepatocytes<sup>26</sup> were seeded in 2ml of Medium 199 (Medium 199 without Phenolred, GIBCO, USA) that contained 10% FCS and 1% antibiotics (Antibiotic-Antimycotic 100X, Life Technologies, USA). Cells were allowed to attach for 2h in an incubator,<sup>30</sup> which maintained a 37°C temperature and an air-humidified atmosphere with 5% CO<sub>2</sub>. Cell confluency was monitored with a light microscope and was typically higher than 90%. After an attachment period of 2h, the medium was replaced by 2.0ml of serum-free Medium 199.

### 3.4 Cytotoxicity model

Cytotoxicity models are frequently used in drug studies. Of major interest are metabolites of drugs and their toxicity.



In contrast to other immortalized hepatic cell lines, primary hepatocytes have the capacity for biotransformation in vitro<sup>25</sup> and, supported by the strategies discussed in section 3.3, are able to maintain their metabolizing activity for a longer time period.<sup>31</sup>

Corresponding to the property of CCl<sub>4</sub> (as a haloalkane) to have a toxic impact on cells by means of bioactivation, primary hepatocytes can be targeted very exclusively, both in vivo and in vitro. Particularly for short-term experiments in vitro, primary hepatocytes are described in the literature as being able to maintain a stable gene expression level of relevant enzymes for bioactivation.<sup>31</sup>

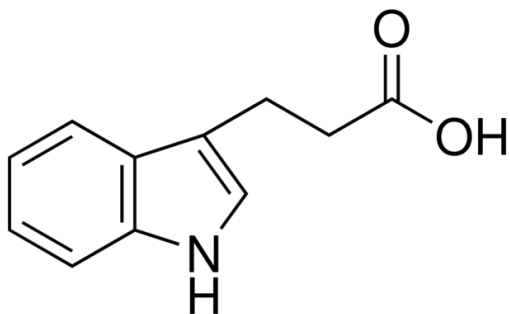
Once CCl<sub>4</sub> was metabolized and the CCl<sub>3</sub>\* radical arose, several mechanisms were seen to have a toxic impact on hepatocytes.<sup>32</sup> The cumulative effect as well as the exclusive impact mediated by lipid peroxidation was measured in this study using several methods such as detecting enzyme leakage, identifying oxidative stress levels, and ascertaining cell death through the microscope.

The pivotal idea to investigate the hepatoprotective effect of IPA required the establishment of CCl<sub>4</sub>-induced cell damage.

#### **3.4.1 Indole-3-propionic acid (IPA)**

Because IPA is a bacterial-derived compound with varying physiological plasma levels in mammals, the concentration of IPA in solution used in this study was ranged mostly from 0.1 μM to 1 μM.

To produce the solution, 0.5mg of IPA stock powder (MP-Biomedicals, USA) were dissolved in 50ml of distilled water. To guarantee a complete dissolving process, sodium hydroxide (c=10M) was added cautiously. Next, the pH was adjusted to 7.00, and the IPA solution was stored at 4°C and protected from light (due to the indole-containing chemical structure as shown in picture 1).



**Picture 1:** structural formula of indole-3-propionic acid (IPA)

### 3.4.2 Carbon tetrachloride (CCl<sub>4</sub>)

To study hepatoprotective effects on primary hepatocytes in vitro, cell damage was induced with hepatotoxic carbon tetrachloride (carbon tetrachloride, reagent grade, 99.9%, 319961 Sigma-Aldrich, USA) within the cell culture.

In the first phase, the cytotoxicity model had to be established. In the second phase, after robust reproducibility of results had been assured, the cytotoxicity model was implemented and valid data could be assessed. Basically, to induce cytotoxicity, CCl<sub>4</sub> was added in a concentration of 10mM to the cell culture.

The haloalkane Carbontetrachloride (CCl<sub>4</sub>) is a colourless liquid characterized by the data sheet given in table 2 (from the producer, Sigma-Aldrich).

**Table 2:** Data sheet of CCl<sub>4</sub> according to Sigma-Aldrich

ACS grade	reagent grade
Vapor density	5.32 (vs air)
Vapor pressure	143 mmHg ( 30 °C) 91 mmHg ( 20 °C)
Assay	99.9%
Refractive index	<i>n</i> <sub>20/D</sub> 1.460(lit.)
Boiling-point	76-77 °C(lit.)
Melting-point	-23 °C(lit.)
Density	1.594 g/mL at 25 °C(lit.)

While performing experiments with CCl<sub>4</sub>, strict safety guidelines had to be followed. All safety instructions for the use of CCl<sub>4</sub> suggested by the manufacturer`s were followed.

#### 3.4.2.1 *Phase 1*

The experimental design was set up based on consideration and evaluation of criteria including the time points of sufficient cell damage induction, the necessary but balanced dose of CCl<sub>4</sub>, and the influence of serum in the culture medium. The cytotoxicity model was established using this methodological approach, and the latest literature was consulted.

As outlined in section 3.2.2, isolated primary hepatocytes were plated in 6-well plates, and after 2h of plating, the medium was changed. Phase 1 experiments were performed changing some wells to Medium 199 containing 0% FCS and some to Medium 199 containing 10% FCS.

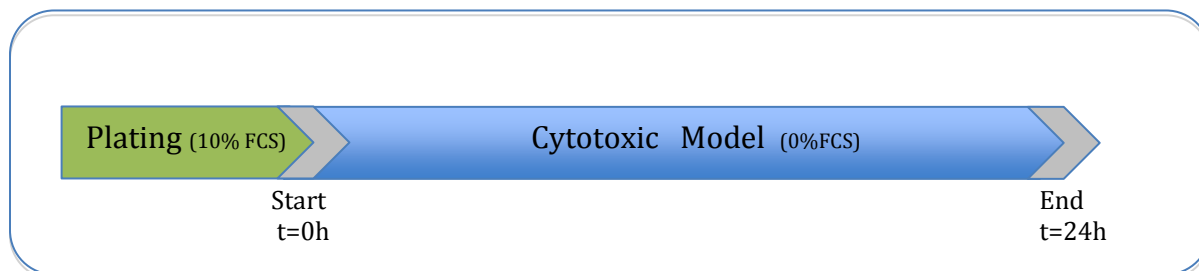
Following standard procedures found in the literature,<sup>33</sup> CCl<sub>4</sub> was diluted to concentrations of 5mM, 10mM, and 25mM by adding the CCl<sub>4</sub> stock solution to the medium in an airtight, lockable, and sterile 50ml conical centrifuge tube (Falcon™ 50ml Conical Centrifuge Tube; Fisher Scientific; USA) directly before use (i.e., directly before adding the new medium to the cell culture well) and shook strongly to support the troublesome dissolving process of CCl<sub>4</sub>. Medium 199 containing CCl<sub>4</sub> and either 0% or 10% FCS was added with sterile 5ml serological pipettes (Corning Costar Stripette, Sigma Aldrich, USA) to the wells with plated hepatocytes. In a literature review, timepoints of 6h and 24h (after adding media containing CCl<sub>4</sub>) were found to be suitable for the needs of this study. With this choice, interference from non-parenchymal cells was also taken into consideration.<sup>34,35</sup>

Finally, 200µl of supernatant was saved for enzyme measurement. The opening of the Eppendorf Pipette tip was placed so that it did not touch the well's wall and was located just beneath the surface of the medium so as not to interfere with the cultured cell monolayer on the bottom of the well. The evacuated supernatant was transferred to capped 1.5ml tubes on ice, and enzyme levels were measured as described in section 3.4.3.

#### 3.4.2.2 *Phase 2*

The preparatory experiments in phase 1, results shown in section 4.2, helped to establish a setup with defined criteria for the cytotoxicity model, and the standard operating procedure (SOP) was maintained as shown in picture 2. A promising configuration for further experiments was defined: a concentration of 10mM CCl<sub>4</sub>, Medium 199 containing 0% FCS and a 24h-treatment period of hepatocytes (compare figures 1 and 2).

In order to fulfil the research community's standards of replicability in experiments, each hepatocyte's treatment was repeated in three wells per isolation, and the mean value of the triplicates was used for further data analysis.



**Picture 2:** Schematic sequence of events defined as standard operating procedure in the cytotoxic model

### 3.4.3 Enzyme leakage

In cytotoxicity evaluation, enzyme leakage of cell cultures in vitro is a commonly used approach. Lactate dehydrogenase (LDH) and alanine aminotransferase (ALT) are primarily of cytosolic origin.<sup>36</sup> The detection of enzyme leakage is performed using a Absorbance-reading device (VersaMax™ ELISA Microplate Reader, Molecular Devices, USA) and corresponding software (SoftMax Pro, Molecular Devices, USA).

#### 3.4.3.1 ALT

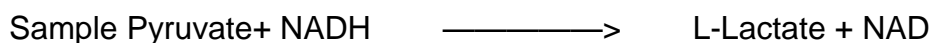
ALT enzyme levels were measured in the supernatant with standards from Document Enzyme Linearity Test Set (Document Enzyme Linearity Test Set, Microgenics Casco Standards, USA).

The applied method for determining ALT was based on recommendations of the International Federation of Clinical Chemistry and Laboratory Medicine (IFCC) and was essentially developed by Bergmeyer,<sup>37</sup> in order to optimize substrate conditions and eradicate side reactions. Linearity of the assay was provided up to 450 U/l depending on the sample-reagent volume quota and the timing of the measurement.

In any ALT measurement, a standard volume of 200µl supernatant from the primary hepatocytes culture was processed. The supernatant was transferred on ice and centrifuged for 2 minutes in order to gather the incidentally aspirated cells into a pellet at the bottom of the tube. With the carefully aspirated 150µl of cell free supernatant, quantitative determination of ALT enzyme levels was conducted.

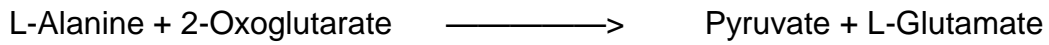
The Infinity ALT Reagent (Infinity ALT (GPT) Liquid Stable Reagent, Thermo Scientific, USA) and optically clear 96-well flat-bottom microplates for absorbance and colorimetric assays were used. Considering the practical challenges caused by the time-dependent character of the enzyme measurement method, 200µl of Infinity ALT Reagent was added to each 20µl of sample contemporaneously using a multi-pipette. In principle, the quantification of ALT enzyme activity in the samples is based on indirect observation. The kinetics of the coenzyme Nicotinamide adenine dinucleotide (NAD) is measured on the basis of changes in the absorbance of light (with a wavelength of 340nm; details are shown in tables 2 and 3). During an initial incubation period after mixing the samples with the Infinity ALT(GPT) Liquid Stable Reagent, the endogenous pyruvate of the samples was rapidly metabolized by LDH. This was anticipated by the producer of the reagent, and offers the advantage of eliminating possible inaccuracy.

LDH:



After a short initial incubation period, any changes of absorbance during the subsequent measurement period are caused by the slower ALT reaction (see section 3.4.3.2) and a subsequent increase in NAD. This can be described in the sequence of the following two enzymatically mediated reactions:

1. ALT:



2. LDH:

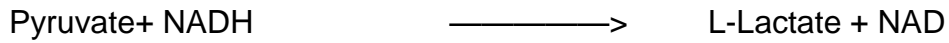


**Table 2:** Reagent Composition of Infinity ALT(GPT) Liquid Stable Reagent

Active Ingredients	Concentration
2-Oxoglutarate	13 mmol/l
L-Alanine	440 mmol/l
NADH	> 0.12 mmol/l
LDH (microbial)	> 2000 U/l
Tris Buffer	97 mmol/l
EDTA	5.0 mmol/l
pH	7.80 ± 0.10 at 20°C.

**Table 3:** System parameters of Infinity ALT(GPT) Liquid Stable Reagent

Temperature	37°C
Primary Wavelength	340 nm
Assay Type	Rate/Kinetic
Direction	Decrease
Sample : Reagent Ratio	1 : 10
used Sample Vol	20 µl
used Reagent Vol	200 µl
Delay/Lag	30 seconds
Read Time	1 to 3 minutes
Linearity	450 U/l

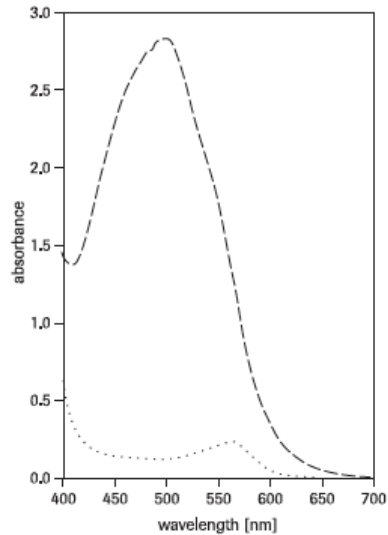
#### 3.4.3.2 LDH

LDH is a stable cytoplasmic enzyme that is present in all cells. Due to the affection of cell membrane integrity, LDH is released into the supernatant of the cell culture. LDH activity (Michaelis constant of periportal LDH in the literature<sup>38</sup>:  $K_M(\text{LDH}) = 8.62\text{-}13.5 \text{ mmol} \times \text{l}^{-1}$ ) in the supernatant was assessed with the Cytotoxicity Detection Kit (LDH, Roche, USA) based on the enzyme kinetic properties of LDH.

After cytotoxicity experiments were performed according to the established model described in section 3.4.2.2, 100µl of cell-free supernatant was transferred to an optically clear 96-well flat bottom microplate well for absorbance and colorimetric assays. To every well containing a sample, 100µl of freshly prepared reaction mixture was added at room temperature. During the 30-minute incubation period, the microplate was protected from light.



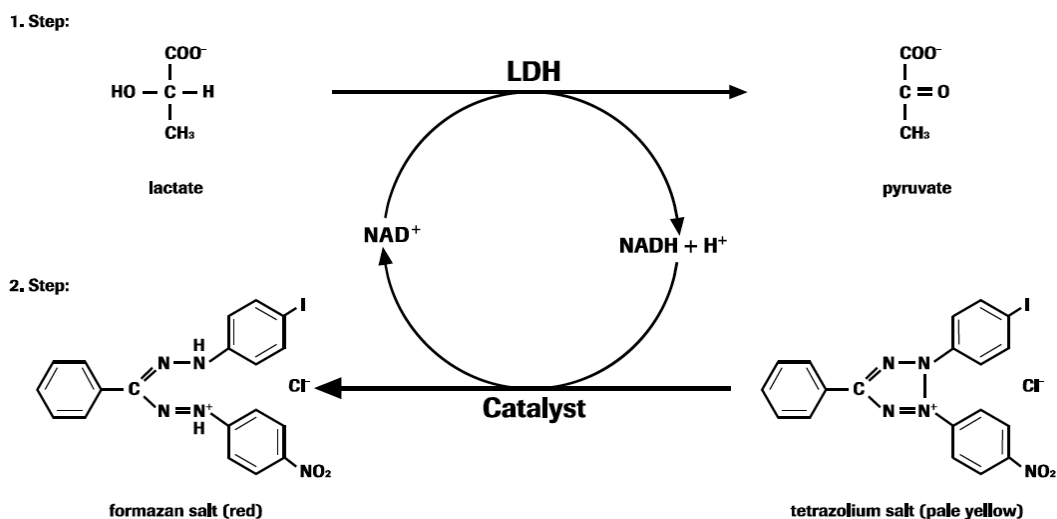
To measure the LDH activity, a spectrophotometric microplate reader captured absorbance at a wavelength of 492nm. Corresponding to pictures 3 and 4 the relationship between LDH activity and absorbance is directly mediated by the amount of formazan formed during a specified time period.



(.....) absence of LDH

(-----) presence of LDH

**Picture 3:** Absorbance spectra of the working solution of the Cytotoxicity Detection Kit added in RPMI 1640 with 1% BSA as published by Roche. (Source: Cytotoxicity Detection Kit (LDH) Manual Version 08)



**Picture 4:** Two-step LDH-mediated reaction with endpoint formazan and coenzyme NAD are shown as published by Roche. (Source: Cytotoxicity Detection Kit (LDH) Manual Version 08)

### 3.4.4 Oxidative stress

Oxidative stress caused by  $\text{CCl}_4$ -initiated radical chain reactions leads to lipid peroxidation. The lipid peroxides are unstable indicators of oxidative stress. Therefore the approach was to measure the aldehydic secondary products of lipid peroxidation as Malondialdehyde (MDA) and 4-hydroxynonenal (4-HNE) by quantifications of their adducts with thiobarbituric acid (TBA).<sup>32</sup>

The oxidative stress was quantified using the OxiSelect™ Thiobarbituric Acid Reactive Substances (TBARS) Assay Kit (Cell Biolabs Inc., USA).

According to the TBARS Assay Kit's protocol, the cell cultures were treated and standardized following the SOP (see section 3.4.2.2). Cell cultures were

harvested from the 6-well plate with 300µl ice-cold phosphate buffered saline (PBS) using a cell scraper. Next, the cultures were centrifuged in a 1.5ml tube for 5 minutes with 600g at 4°C, and finally they were resuspended with PBS containing 0.05% butylated hydroxytoluene (BHT) for ultrasonic comminution conducted on ice. The whole homogenate was further used in the assay. A standard curve was produced using Malondialdehyde bismethylacetal (MDA) ranging from 0M to 125µM (see table 4). Cell homogenate was also treated with SDS Lysis Solution for 5 minutes at room temperature in order to disrupt the cell membranes. Each cell homogenate was incubated with TBA Reagent in the heatblock at 95°C for 45 to 60 minutes and cooled again on ice to room temperature. Samples were centrifuged again at 3000rpm for 15 minutes and supernatant was collected for extraction of TBARS by butanol (n-Butanol, Sigma-Aldrich, USA) to prevent interference with hemoglobin and its derivatives. Fluorescence measurement was performed using black 96-well flat bottom microplates for fluorescent assays. The fluorescence of duplicates of both samples and standards were measured as recommended by the manufacturer's instructions.

**Table 4:** MDA Standard - Curve

<b>MDA Standard (µM)</b>
125
62.5
31.25
15.63
7.81
3.91
1.95
0.98
0.0

### 3.5 Western Blot

The Western Blot technique was described separately by Renart and Towbin in 1979.<sup>39,40</sup> The protein is presented on a nitrocellulose paper and can be stained, allowed to react with antibodies, and be cleaved proteolytically or chemically.<sup>41</sup>

#### 3.5.1 Homogenization of protein extracts

Directly after the incubation period, the lysate from the cell cultures was produced.

The hepatocyte culture dish was transferred from the incubator to ice and washed twice with ice-cold PBS. Adherent cells were scraped off the well's bottom and prepared for Western Blot analysis with the lysis buffer Dignam C (see table 5) containing freshly added Protease (Roche) and Phosphatase inhibitors (Sigma). This is done to disrupt cell membrane, solubilize intracellular proteins, and slow down the proteolysis, dephosphorylation, and denaturation that usually occur after lysis.

**Table 5:** Recipe of lysis buffer Dignam C

HEPES pH 7.9	10mM
NaCl	0.42M
MgCl <sub>2</sub>	1.5mM
DTT	0.5mM
Glycerol	2.5ml
NP-40	50µl
ddH <sub>2</sub> O	6.49ml
Proteinase inhibitor	1 tablet
Phosphatase inhibitor (100x)	10

### 3.5.2 Protein concentration

Protein concentration was assessed using the common bicinchoninic acid (BCA) assay (Pierce™ BCA Protein Assay Kit, Thermo Scientific, USA).<sup>42,43</sup> The assay is based on the reduction of copper ( $\text{Cu}^{2+}$  to  $\text{Cu}^{+}$ ) and is followed by BCA chelation as well as complex formation. This reaction results in a color change from green to purple, which can be measured photometrically with absorbance at a wavelength of 560nm.<sup>44</sup>

With the BCA standards ranging from 0 to 10  $\mu\text{g/l}$ , the protein concentration of the samples was determined by linear regression. Therefore, standards and samples were run in duplicates on the same optically clear 96-well flat-bottom microplate for absorbance and colorimetric assays.

In preparation for the assays, 200 $\mu\text{l}$  BCA Protein Assay Mix was added to 5 $\mu\text{l}$  of homogenates of the cell culture extracts with the multi pipette. After an incubation period of 30 minutes at 37°C, absorbance was measured and protein concentration calculated for further experiments.

### 3.5.3 Gel production

The separating gel was mixed, according to the protein size of interest, as described in tables 6 and 7.

In detail, glass frames for polyacrylamide gels were prepared by cleaning two 10cm x 10cm pieces of glass plate with 70% ethanol. The plates were assembled with spacers in between. Next 80% of the space in the frame was filled with separating gel, and the height of the solution was marked on the outside of the frame. TEMED (Tetramethylethylenediamine, Sigma-Aldrich, USA) and 10% APS (Ammonium Persulfate, Sigma-Aldrich, USA) start the polymerisation of Acrylamide and were added just before use. To produce an

even surface on the separating gel, 0.3ml of ddH<sub>2</sub>O was added carefully in a thin continuous separating line on top of the separating gel solution after the upright standing glass frame was filled. When the polymerization was finished, ddH<sub>2</sub>O was finally shed off.

The stacking gel was produced following a recipe: 3.2ml ddH<sub>2</sub>O, 1.25ml 0.5M Tris (Tris-buffered saline, Sigma, USA) pH 6.8, 50µl 10% SDS (sodium dodecyl sulfate, USA), and 0.5ml Acrylamide 40% (Acrylamide 40%, USA). The gel was mixed, and just before use 25µl of 10% APS and 10µl of TEMED were added.

The stacking gel was poured carefully onto the already solidified separating gel and a 14-tooth comb was inserted into the stacking gel solution. After the gels were solidified completely, the glass frame with the gels was fit into an electrophoresis chamber. The comb was removed carefully to create undamaged pockets, which were checked by rinsing the pockets with a running buffer solution (containing Tris, Glycine, and SDS). The electrophoresis chamber was filled with running buffer solution.

**Table 6:** Acrylamide percentage dependent on size of protein of interest

<b>Percentage Acrylamide</b>	<b>Protein Size</b>
15%	<17kDa
12%	17–30kDa
10%	30–70kDa
7.5%	70–94kDa
5%	94– 212kDa

**Table 7:** Content of separating gel dependent on protein size (compare table 6)

Separating Gel	15%	12%	10%	7.5%	5%
ddH <sub>2</sub> O	3.5mL	4.3ml	4.8mL	5.4mL	6.1mL
<u>1.5M Tris pH 8.8</u>	2.5mL	2.5mL	2.5mL	2.5mL	2.5mL
10% SDS	100µL	100µL	100µL	100µL	100µL
Acrylamide <u>40%</u>	3.8mL	3mL	2.5mL	1.9mL	1.25mL
<i>Add right before use:</i>					
10% APS	50µL	50µL	50µL	50µL	50µL
TEMED	20µL	20µL	20µL	20µL	20µL

### 3.5.4 Electrophoresis

In gel electrophoresis proteins are separated by size. To prepare proteins for SDS-PAGE (sodium dodecyl sulfate polyacrylamide gel electrophoresis), Loading Buffer (NuPAGE LDS Sample buffer (4X), Life Technologies, USA) was added to the samples and they got denatured and coupled with negative charge by means of 5 minutes heating at 95°C in a heatblock. The amount of sample protein was set as 50µg of proteins per pocket. Therefore, a corresponding volume of the sample protein was calculated after measuring the protein concentration (as described in section 3.5.2) and added to a capped 1.5ml tube. Subsequently, proteins were added carefully to the gel pockets. Additionally, one pocket was loaded with 5µl of PageRuler Ladder (Page Ruler Prestained Protein Ladder, USA) to help determine the size of the sample proteins.

In the electrophoresis process, voltage was first set to 110V. When the PageRuler Ladder reached the marked borderline of stacking and separating gel, the voltage was upregulated to 130V until the lowest molecular-weight marker reached the bottom of the gel.

### 3.5.5 Blotting

To detect proteins in additional experiments, they were transferred to a membrane using a semi-dry blotting transfer method.<sup>45</sup> Thick and thin Whatman papers and nitrocellulose paper were moistened with Transfer Buffer Mix (TBM) containing methanol. Gel was taken out of the glass frame using a thin Whatman paper. The materials on the Trans-Blot Cassette were arranged in the following order from bottom to top: thick Whatman paper, thin Whatman paper, nitrocellulose membrane, gel, thin Whatman paper, and thick Whatman paper. Applying 15V to the Trans-Blot Cassette, the proteins were blotted in 30 minutes from the gel to the nitrocellulose membrane. After a Ponceau S (Sigma- Aldrich, USA) staining, the protein lanes were visible and the nitrocellulose membrane was cut for further experiments and washed twice in ddH<sub>2</sub>O. For blocking, the nitrocellulose membrane was incubated for 60 minutes in 5% milk [containing 2.5g fat-free milk powder (Non Dry Fat Milk, Sigma, USA), 25ml TBST, 25 ml ddH<sub>2</sub>O].

### 3.5.6 Immunostaining

Proteins of interest were visualized for further analysis using immunostaining technique. In short, a primary antibody that binds to a specific protein epitope is detected by a secondary, horseradish-peroxidase-labelled antibody. A chemiluminescent substrate for horseradish peroxidase (HRP) is applied and the nitrocellulose membrane is exposed to an X-ray film. For washing nitrocellulose membrane, TBST [Tris-Buffered Saline containing 0.1% Tween 20 (Sigma- Aldrich, USA)] was used.

The primary antibody (β-actin: monoclonal anti-beta-actin, clone ac-15, Sigma- Aldrich, USA; CYP2E1: anti-CYP2E1, ab1252, Fisher Scientific, USA; SOD1: sheep anti-human superoxide dismutase, pc077, The Binding Site, UK;<sup>46</sup> HSP27: HSP27 (C-20), sc-1048, Santa Cruz Biotechnologies, USA) was diluted



according to the manufacturer's instructions in 5% milk, and nitrocellulose was incubated for 1h or overnight at 4°C. After thorough rinsing with TBST the corresponding secondary antibody, labelled with HRP, was diluted according to the manufacturer's instructions in 10ml of 5% milk, and nitrocellulose was incubated for 30 to 60 minutes and afterwards was rinsed again for 20 minutes with TBST.

For chemiluminescence, the membrane was incubated with 1.5ml SuperSignal solution (SuperSignal™ West Pico Chemiluminescent Substrate, Thermo Fisher Scientific, USA) for 5 minutes. Afterwards, the membrane was cleared of SuperSignal solution, wrapped in transparent polyethylene film and exposed for 5 minutes to an X-ray film in an autoradiography cassette (Fisher Biotech Autoradiography Cassette, fbxc-810, Fisher Scientific, USA). Visibility and darkness of the protein lanes on the film (Blue X-Ray Film, 5 x 7, Phenix Research Products, USA) were appraised, and the exposure time was adjusted dependently.

### 3.5.7 Densitometry

The used densitometric method is based on the absorbance of light, which depends on the darkness of the X-ray film. Light was partly absorbed, and the decrease of incident light was measured electronically in a determined quantitative dynamic range for each target protein. The constitutively expressed housekeeping gene  $\beta$ -actin was used as a loading control and served to normalize the loading of the protein of interest. Western blots with an overloading of  $\beta$ -actin were excluded from the densitometrical analysis, and equal expression levels of  $\beta$ -actin in different experimental conditions were assured.<sup>47</sup>

## 3.6 Statistical Analysis

### 3.6.1 Image analysis

All image analysis was performed with open-source NIH-ImageJ software (ImageJ 1.47f; National Institute of Health, USA).

### 3.6.2 Statistical analysis

The Mann–Whitney U rank-sum test was used for statistical analysis (Prism, GraphPad Software, Incorporated, La Jolla, CA, USA). Data are presented as mean  $\pm$ SD, and a level of significance  $P \leq 0.05$  was selected.

## 4 Results

All primary hepatocytes were isolated as described in section 3.2 from C57BL/6 background wild-type mice with a minimum age of 6 weeks. Primary hepatocytes were used instead of immortalized cell lines to exploit the most representative in vitro model for physiological processes.

The viability was measured prior to experiments by Trypan Blue exclusion. The average viability of primary hepatocytes used in our experiments was 75.25 %.

#### 4.1 Impact of IPA on primary hepatocyte cultures

IPA was tested in different concentrations (exceeding physiologically measured concentrations of mammalian plasma) in primary hepatocyte cultures, and its effect on cell viability was evaluated by ALT release.

IPA was used in concentrations of 0.1 $\mu$ M, 1 $\mu$ M, 10 $\mu$ M, and 100 $\mu$ M. The ALT enzyme activity levels in the supernatant were compared to a control group.<sup>19</sup> Every condition was plated in duplicate in 6-well plates with Media 199 containing 0% FCS and incubated for 24h.

There was no significant difference or trend between the control group and the IPA-treated conditions in the leakage of ALT (data not shown).

Taken together, no hepatotoxic effect caused by the bacteria-derived compound IPA was visible. Primary hepatocytes showed neither any microscopically observable sign of additionally induced cytotoxic impact nor higher rates of detachment in vitro due to IPA.

#### 4.2 Cytotoxicity model

To study hepatoprotective effects on primary hepatocytes, cell damage was induced with hepatotoxic CCl<sub>4</sub>. As described in section 3.4.2.3, cells were attached in a monolayer to the collagen-coated plate for 2h in a medium containing 10% FCS. Next, the media was changed to one containing either 10% or 0% FCS.<sup>30,48</sup>

In accordance with relevant literature, CCl<sub>4</sub> was applied in concentrations of c(CCl<sub>4</sub>)=5mM, 10mM, and 25mM.<sup>33</sup> To evaluate the dynamics of cell damage, different time points (6h and 24h after the start of CCl<sub>4</sub> treatment) were set for measurement as shown in figure 1(A). Fatal cell damage causing ALT release, among other things, caused by the disintegration of cell membrane, was evaluated by the ALT enzyme activity in the supernatant (figure 1A).<sup>49</sup>

Fluorescence microscopy was performed after cells were stained with Hoechst and Propidium Iodide.<sup>50</sup> Structural changes, especially signs of apoptosis and necrosis, were evaluated and found to be higher after 24h in randomly captured pictures of CCl<sub>4</sub>-treated conditions compared to the control (picture 5).

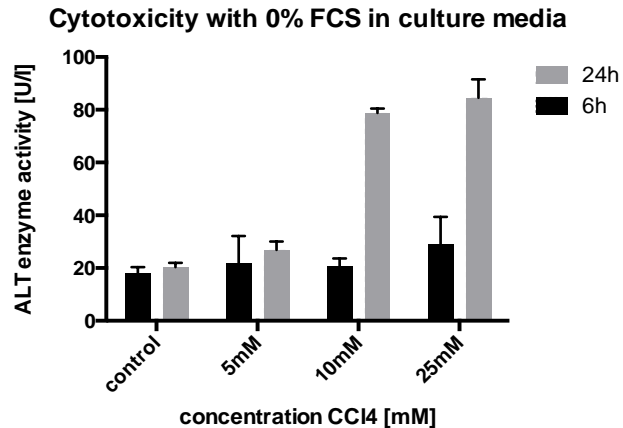


**Figure 1(A): Cytotoxicity of different CCl<sub>4</sub> concentrations with no serum proteins.** 900.000 cells were plated per well (growth area 1.6 cm<sup>2</sup>) with  $n=3$  wells per condition. No FCS was added to the culture media. ALT enzyme activity levels are shown after 6h and 24h. Mean values are shown with SD.

As shown in the figure 1(A), the control with 0% FCS showed no substantial increase of ALT. Mean ALT enzyme activity in the control after a period of 6h was  $A(\text{ALT},6\text{h})= 17.90$  U/l, and no change was evident after 24h ( $A(\text{ALT},24\text{h})=20.40$  U/l).

Promising results for establishing a cytotoxicity model were obtained with 0% FCS and  $c(\text{CCl}_4)=10\text{mM}$ . No evident difference to the control was seen after a period of 6h with  $A(\text{ALT},6\text{h})= 20.60$  U/l, but a four-fold increase of the transaminase activity level after 24h to  $A(\text{ALT},24\text{h})= 78.8$  U/l could be detected.

Additional fluorescence microscopy data revealed a loss in cell plasma membrane integrity, particularly propidium iodide uptake, within 18.8% of primary hepatocytes after 24h.

A closer look at the condition 0% FCS treated with 25mM CCl<sub>4</sub> revealed the most promising cytotoxic impact after both 6h and 24h. The fluorescence microscopy showed that 32.01% of the cells were positive for propidium iodide after 24h.

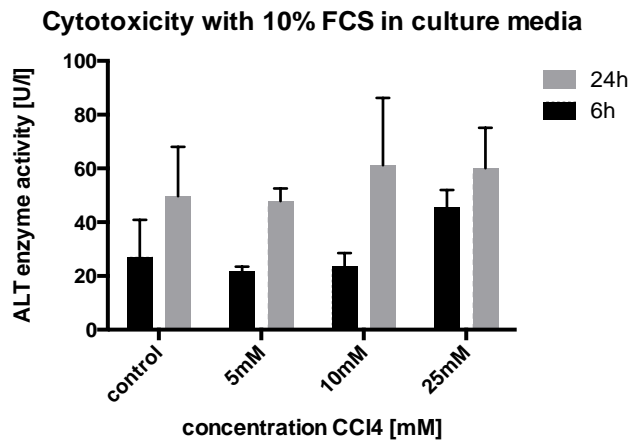


**Figure 1(B): Cytotoxicity of different CCl<sub>4</sub> concentrations with 10% FCS.**

900.000 cells were plated per well (growth area 1.6 cm<sup>2</sup>) with *n*=3 wells per condition. 10% FCS was added to the culture media. ALT enzyme activity levels are shown after 6h and 24h. Mean values are shown with SD.

Figure 1(B) shows primary hepatocytes treated for 24h with Media 199 containing 10% FCS and varying concentrations of CCl<sub>4</sub>.<sup>51</sup>

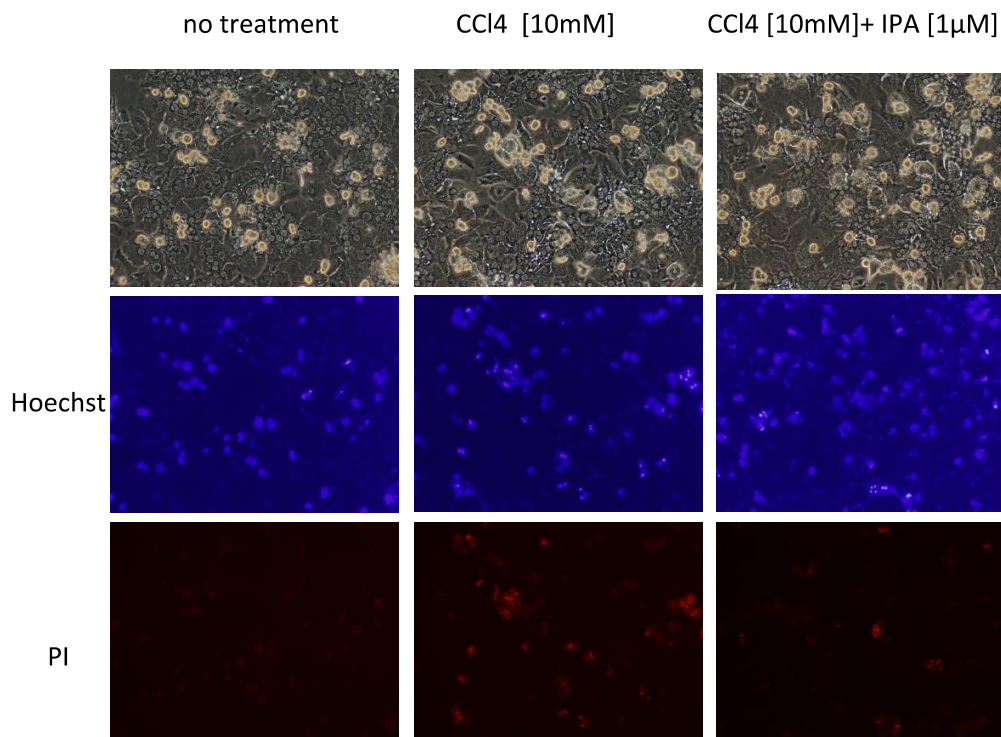
In the control, ALT levels rose after 6h from A(ALT,6h)= 27.10 U/l to A(ALT,24h)=49.68 U/l after 24h. In the supernatant of the cell culture treated with c(CCl<sub>4</sub>)=10mM, the 6h ALT activity level was A(ALT,6h)=23.59 U/l, and it rose to A(ALT,24h)=61.24 U/l after 24h. With a concentration of c(CCl<sub>4</sub>)=25mM, the 6h value result of the ALT level was already A(ALT,6h)=45.50 U/l.

Distilled, any robust increase in ALT enzymes released into the supernatant was found after 24h with the media containing 10% FCS.

### 4.3 Hepatoprotective effect of IPA

#### 4.3.1 First impression by dye uptake

A first attempt to estimate the hepatoprotective potential of IPA was staining with Hoechst and propidium iodide. A promising hepatoprotective effect was a first rationale for further investigation. As exemplarily shown in picture 5, lower dye-uptake after 24h was presented by hepatocytes, when an additional 1 $\mu$ M of IPA was applied to the medium.



**Picture 5:** Light/Fluorescence microscopy of primary hepatocytes cultured for 24h in 6-well plates under following condition: no treatment; 10mM CCl<sub>4</sub>; 10mM CCl<sub>4</sub>, and 1 $\mu$ M IPA.

### 4.3.2 CYP2E1 levels

The cytochrome P450 system in hepatocytes is mainly responsible for the oxidative metabolism of xenobiotics as drugs or bacteria-derived toxic compounds. The CYP450 enzymes helped to estimate the maintenance of differentiation in the cultured primary hepatocytes.<sup>52</sup>

CYP2E1 is the primary enzyme involved in the degradation of CCl<sub>4</sub> to the reactive and toxic trichloromethyl radical (CCl<sub>3</sub>\*), and it mediates the detrimental effect in CCl<sub>4</sub> treatment.<sup>32,53-55</sup>

In *n*=3 experiments (see figure 2) primary hepatocytes in 6-well plates with 900,000 cells per well for 24h in media containing 0% FCS following the SOP were cultured. Each condition was cultured in triplicate, whole protein extracts were pooled, and immunoquantification was performed by SDS-PAGE with the antibody described in section 3.5.

CYP2E1 protein expression level was normalized with β-actin as a loading control.<sup>56</sup> No significant difference in the expression of CYP2E1 occurred. Nevertheless, an apparent trend in protein level could be characterized as a 4-fold decrease in conditions with CCl<sub>4</sub> alone. With the presence of 0.1 μM IPA, only a 2-fold decrease of CYP2E1 after treatment with CCl<sub>4</sub> for 24h (0.58 fold control) was quantified. Subsequently, with 10 mM of CCl<sub>4</sub> and an IPA concentration of 1 μM, even a 1.76-fold increase of CYP2E1 protein expression level after 24h compared to the control condition was observed. A 1.18-fold increase with 0.1 μM IPA alone and a questionable dose-dependent 1.44-fold increase with 1 μM IPA alone was found.

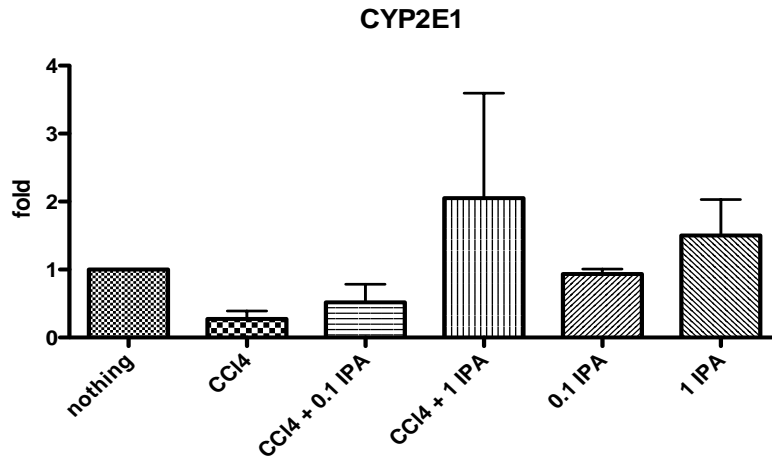


**Figure 2: Equal bioactivation of CCl<sub>4</sub> with and without IPA.**

In  $n=3$  experiments primary hepatocytes were cultured for 24h under each condition in triplicate. CCl<sub>4</sub> concentration was 10mM and IPA concentrations were 0 $\mu$ M (nothing), 0.1 $\mu$ M, and 1 $\mu$ M. CYP2E1 protein levels were identified by normalizing to  $\beta$ -actin and are shown in comparison to the control condition. Mean values are shown with SD.

#### 4.3.3 Cell damage marker levels in vitro

Figures 3–5 summarize and quantify the cell damage caused by various mechanisms of CCl<sub>4</sub>-mediated cytotoxicity in primary hepatocyte cultures after 24h of treatment with and without IPA treatment.



#### 4.3.3.1 ALT enzyme leakage

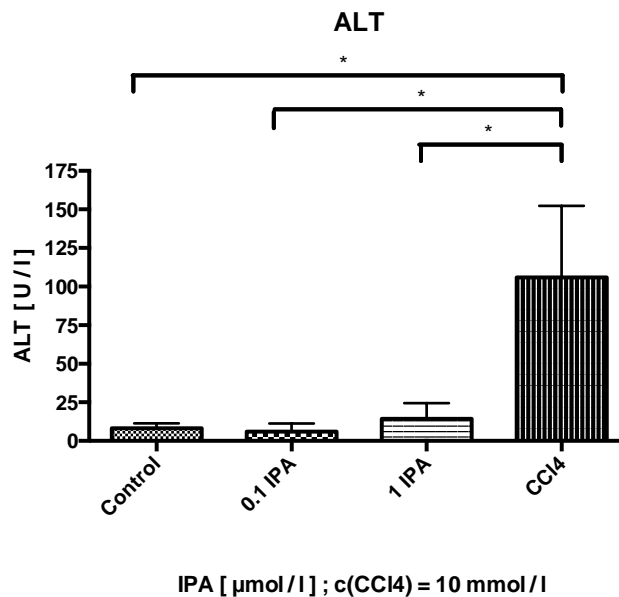


**Figure 3(A) Impact of IPA on ALT enzyme leakage.**

$9 \times 10^5$  hepatocytes were cultured as described in section 3.4 and treated with IPA-concentrations of  $0\mu\text{M}$  (control),  $0.1\mu\text{M}$ , and  $1\mu\text{M}$  and are compared to treatment with  $\text{CCl}_4$ . In  $n=8$  independent isolations, each condition was performed in triplicate. Absolute enzyme-activity of ALT in the medium after 24h was measured. Mean values are shown with SD.

In figure 3(A), ALT levels in the culture media are shown. Under control conditions, the enzyme activity after 24h in the culture media was significantly lower ( $P= 0.0002$ ) than after  $\text{CCl}_4$  treatment. Furthermore, hepatocytes treated with  $0.1\mu\text{M}$  ( $P= 0.0002$ ) and  $1\mu\text{M}$  ( $P=0.0019$ ) IPA showed significantly lower enzyme activity than the  $\text{CCl}_4$ -treated cells.

Treating only with IPA did not show significant differences compared to the control group.

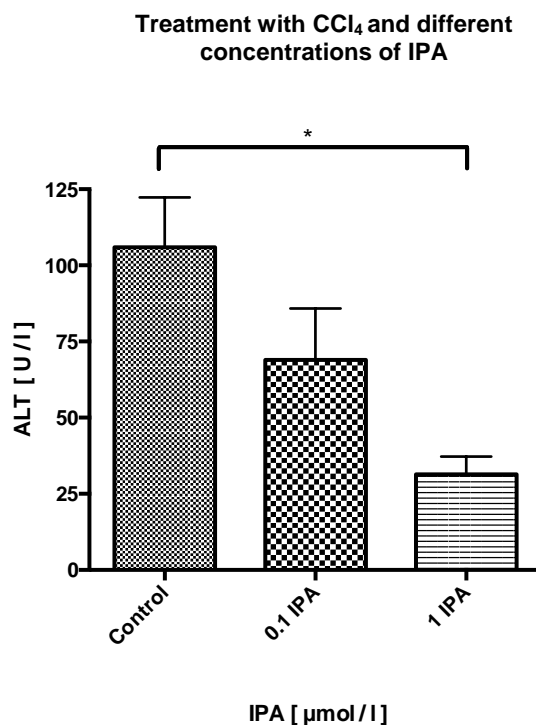


**Figure 3(B): Protective effect of IPA on hepatocytes (dose dependent) after CCl<sub>4</sub> treatment.**

9 x 10<sup>5</sup> hepatocytes were cultured as described in section 3.4 and treated with CCl<sub>4</sub> and IPA-concentrations of 0μM (control), 0.1μM, and 1μM. In *n*=8 independent isolations each condition was performed in triplicate. Absolute enzyme activity of ALT in the medium after 24h was measured. Mean values are shown with SD.

In Figure 3(B), ALT levels in the culture media after 24h of treatment with CCl<sub>4</sub> were measured. Interestingly, the data show a dose-dependent decrease of ALT enzyme leakage with rising IPA levels. Mean ALT levels in the control condition declined with treatment of 0.1μM IPA and further decreased significantly (*P*=0.0047) with 1μM IPA compared to the control condition, which was solely treated with CCl<sub>4</sub>.

#### 4.3.3.2 LDH enzyme leakage

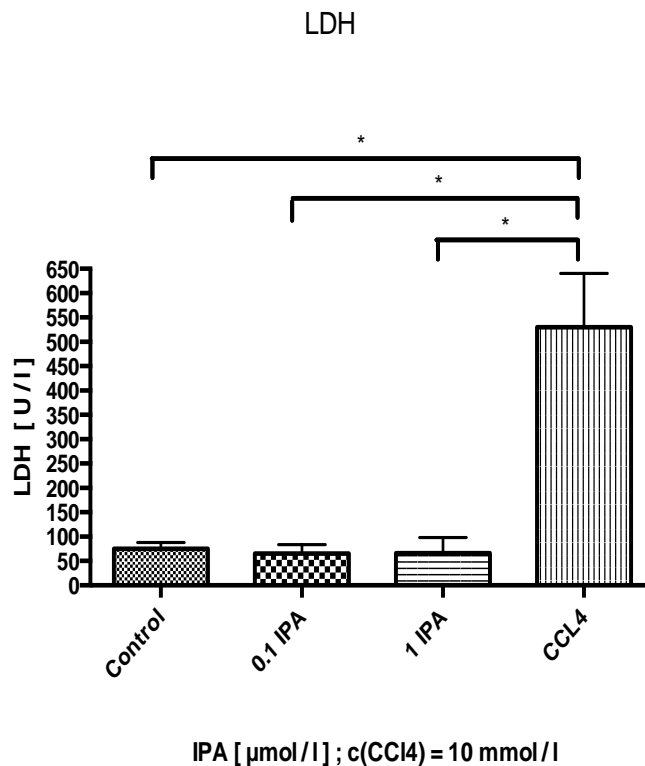


**Figure 4(A): Impact of IPA on LDH enzyme leakage.**

Using the method described in section 3.4,  $9 \times 10^5$  hepatocytes were cultured and treated with IPA concentrations of  $0\mu\text{M}$  (control),  $0.1\mu\text{M}$ , and  $1\mu\text{M}$  and are compared to treatment with  $\text{CCl}_4$ . In  $n=6$  independent isolations, each condition was performed in triplicate. Absolute enzyme-activity of LDH in the medium after 24h was measured. Mean values are shown with SD.

In Figure 4(A), LDH levels in the culture media were measured. After 24h enzyme activity found in the control sample was significantly lower ( $P= 0.0022$ ) than after  $\text{CCl}_4$  treatment.

Moreover, conditions treated with  $0.1\mu\text{M}$  ( $P= 0.0022$ ) and  $1\mu\text{M}$  ( $P= 0.0043$ ) of IPA caused significantly lower enzyme activity than the  $\text{CCl}_4$ -treated condition in the supernatant.

Addition of IPA alone did not lead to significant differences in LDH enzyme activity levels compared to the control group.

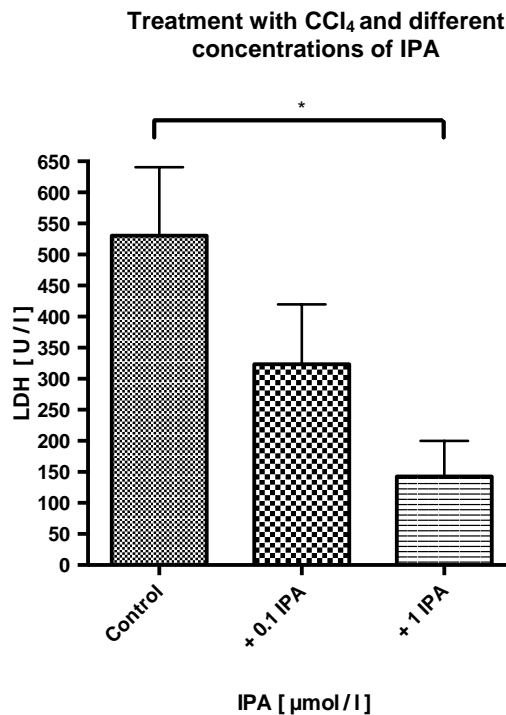


**Figure 4(B): Protective effect of IPA on hepatocytes (dose dependent) after CCl<sub>4</sub> treatment.**

As described in section 3.4,  $9 \times 10^5$  hepatocytes were cultured and treated with CCl<sub>4</sub> and IPA-concentrations of 0μM (control), 0.1μM, and 1μM. In  $n=6$  independent isolations each condition was performed in triplicate. Absolute enzyme activity of LDH in the medium was measured after 24h. Mean values are shown with SD.

In Figure 4(B), treatment of hepatocytes with carbon tetrachloride ( $c(\text{CCl}_4)=10\text{mmol/l}$ ) for 24h prior to the observations of enzyme levels was performed for every condition.

As the IPA dose was increased to 1 μM, the leakage of enzymes could be reduced to a significant difference compared with the control.

#### 4.3.4 Oxidative stress in primary hepatocytes in vitro

Oxidative stress was measured as described in section 3.4.4 from whole cell extracts using the OxiSelect TBARS assay. TBARS quantifies ROS indirectly and is shown in the figures in arbitrary units.<sup>57</sup>

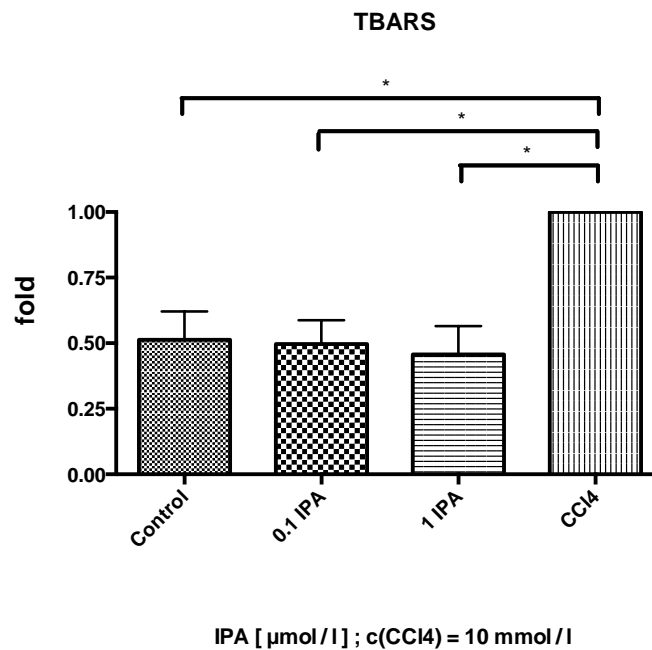


#### Figure 5(A): Oxidative stress in hepatocytes is reduced by IPA.

As described in section 3.4,  $9 \times 10^5$  hepatocytes were cultured and treated with IPA-concentrations of  $0\mu\text{M}$  (control),  $0.1\mu\text{M}$ , and  $1\mu\text{M}$  and are compared to treatment with  $\text{CCl}_4$ . In  $n=7$  independent isolations each condition was performed in triplicate. Mean values are shown with SD.

As shown in Figure 5(A), the TBARS were significantly induced by treatment of primary hepatocytes with 10mM of toxic  $\text{CCl}_4$  in relation to the baseline of the control or to IPA treatment. IPA treatment did not alter the TBARS concentration after 24h compared to the control significantly.

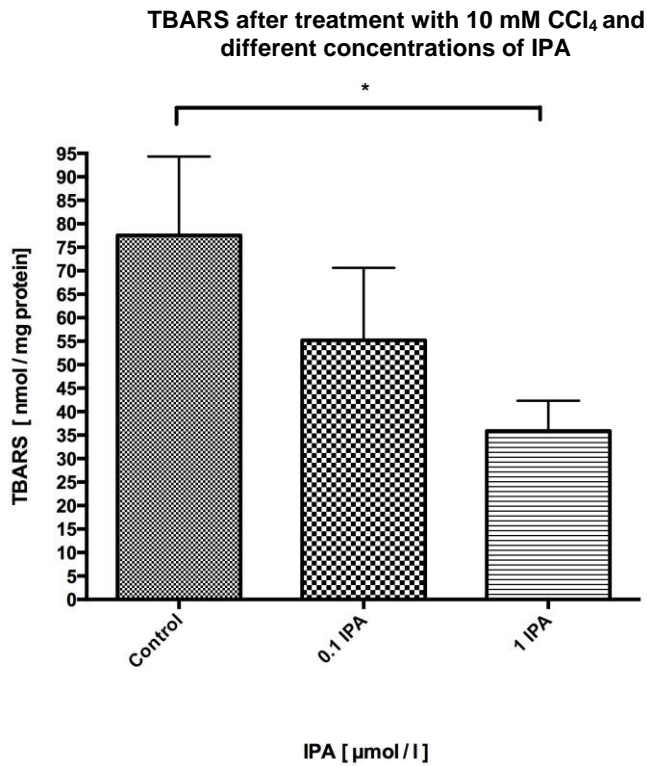


**Figure 5(B): Oxidative stress is reduced in hepatocytes by IPA.**

As described in section 3.4,  $9 \times 10^5$  hepatocytes were cultured and treated with CCl<sub>4</sub> and IPA-concentrations of 0μM (control), 0.1μM, and 1μM. In  $n=4$  independent isolations each condition was performed in triplicate. Mean values are shown with SD.

To validate IPA's potential of reducing the toxic impact of CCl<sub>4</sub>, TBARS were measured in hepatocyte cultures simultaneously treated with 10mM CCl<sub>4</sub> and treated with IPA. TBARS decreased with IPA treatment dose dependently as shown in Figure 5(B). A significant decrease of TBARS could be assessed with 1μM IPA treatment compared to treatment with CCl<sub>4</sub> alone.

## 4.4 Role of IPA in hepatic metabolism in addition to antioxidant properties

The rationale for further screening of protein induction by IPA was the protective properties of IPA in mammalian metabolism. As the first attempt of Venkatesh et al. suggests, IPA was found to serve as a PXR ligand and likely influences TNF- $\alpha$  and mRNA levels, and protein expression in enterocytes in vivo.

Sakurai et al. investigated the pathways of compensatory proliferation and liver tumor promotion. They paid attention to the effect of ROS accumulation in hepatocarcinogenesis and found, downstream of p38 $\alpha$ , that HSP27 has an antioxidant effect associated with its ability to restore reduced Glutathione (GSH) and compensate the toxic effect of oxidized proteins leading to less ROS but JNK-mediated compensatory proliferation. Another route, downstream of IKK $\beta$  and NF- $\kappa$ B, superoxide dismutase (SOD) was defined as a critical antioxidant.<sup>58</sup>

### 4.4.1 SOD1

As a housekeeping antioxidant protein, SOD1 reduces superoxide in hydrogen peroxide, which is further metabolised by other proteins.<sup>59-62</sup>

## SOD1

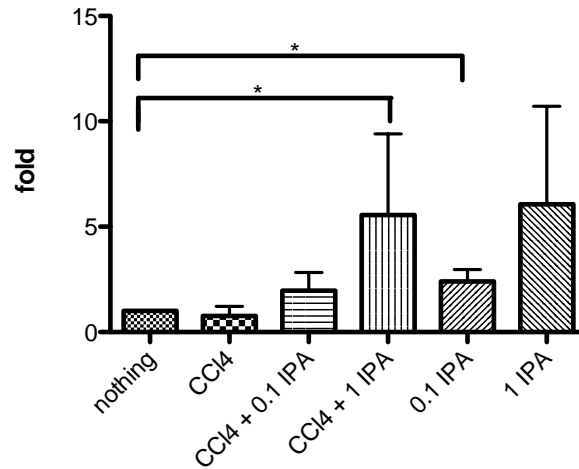


**Figure 6: relative SOD1 protein levels in hepatocytes.**

Protein levels were assessed using a Western Blot analysis. As described in section 3.4,  $9 \times 10^5$  hepatocytes were cultured and treated with CCl<sub>4</sub> (c=10mM) and IPA-concentrations of 0 $\mu$ M (nothing), 0.1 $\mu$ M, and 1 $\mu$ M for 24h. In  $n=4$  independent isolations each condition was performed in triplicate. Mean values are shown with SD.

SOD1 protein concentration normalized to the housekeeping gene  $\beta$ -actin was assessed using a Western Blot analysis and densitometry. Results are expressed in relation to a control untreated hepatocyte culture.

SOD1 was found to be upregulated to a significant extent.

After exposure to the impact of free radicals, stemming from the bioactivation of 10mM CCl<sub>4</sub> in the primary hepatocytes culture, significant SOD1 upregulation could be observed when 1 $\mu$ M IPA was applied simultaneously to the cell culture.



SOD1 was significantly induced under solely 0.1 $\mu$ M IPA treatment compared to the control (Figure 6).

#### 4.4.2 HSP27

Chaperones such as HSP 27 provide an important antiapoptotic and antioxidant function.<sup>63</sup> The metabolic regulation of chaperones is not completely understood at this time.<sup>64</sup>

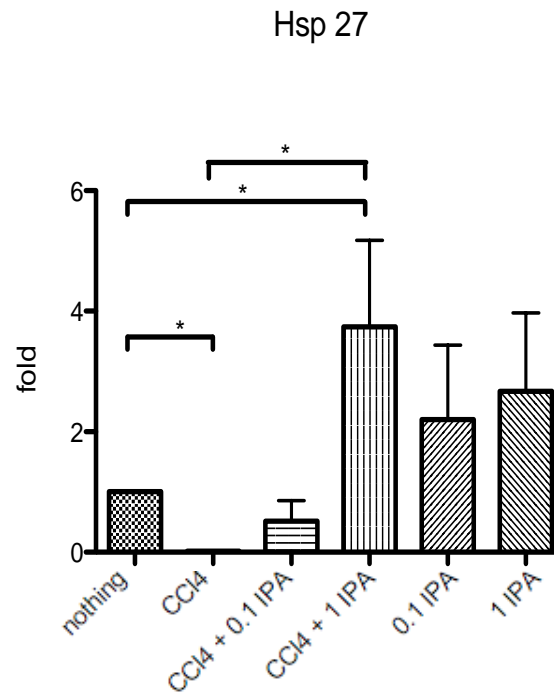


**Figure 7: relative HSP27 protein levels in hepatocytes.**

Protein levels were assessed with a Western Blot analysis. As described in section 3.4,  $9 \times 10^5$  hepatocytes were cultured and treated with CCl<sub>4</sub> (c=10mM) and IPA-concentrations of 0 $\mu$ M (nothing), 0.1 $\mu$ M, and 1 $\mu$ M for 24h. In  $n=4$  independent isolations each condition was performed in triplicate. Mean values are shown with SD.

In primary hepatocytes, the baseline HSP27 protein concentration of the control was compared to treatment with 10 mM CCl<sub>4</sub> and is found to be significantly reduced to very low levels. Evidently, HSP27 was restored with IPA treatment.

When a dose of 1 μM IPA is applied during treatment with CCl<sub>4</sub>, the total HSP27 protein expression in vitro is significantly higher than under CCl<sub>4</sub> alone. Interestingly, with IPA treatment alone, HSP27 was induced more than 2-fold.

Considering these results, the potential of using IPA to induce HSP27 was hypothesized. In a subsequent experiment, IPA was applied in a linearly increasing concentration with a range of up to 100 μM.

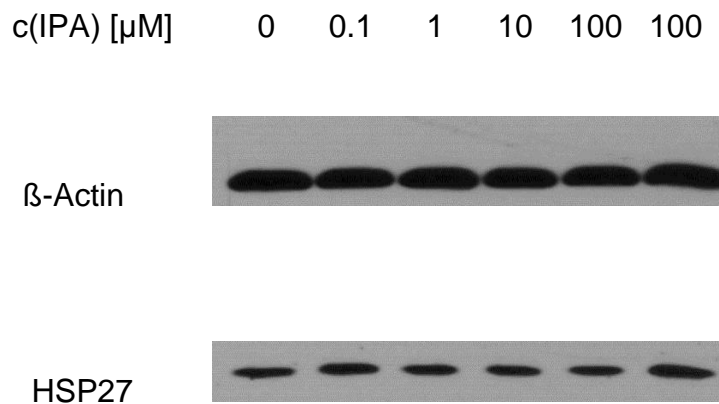


**Figure 8: Protein levels of HSP27 after IPA stimulation in hepatocytes.**

9 x 10<sup>5</sup> cells per well were stimulated for 24h with IPA in the concentrations of 0 μM, 0.1 μM, 1 μM, 10 μM, and 100 μM. β-actin was used as loading control. N=4 in separate experiments.

As shown in figure 8, all lanes were equally loaded assuring representative results for HSP27 protein expression. No change in HSP27 protein expression could be observed under any concentration of IPA treatment alone.

## 5 Discussion

The present study was designed to determine the effect of IPA on primary hepatocytes. It found a dose-dependent hepatoprotective effect of IPA on primary hepatocytes in vitro. In the study design, the regenerative capacity of hepatocytes was challenged with hepatotoxic CCl<sub>4</sub>, which is commonly used in liver research.

The antioxidant activity of IPA, particularly its hydroxyl radical scavenging potential, has been investigated by Chyan et al. and compared to other potent radical scavengers, such as vitamins C and E or glutathione, no pro-oxidant intermediates were found to be built with IPA.<sup>19</sup>

Accordingly, IPA was used up to a maximum concentration of 100µM and showed no harmful impact in cultures of primary hepatocyte. Quantification of the pH shift was found to be unnecessary due to the low concentrations of IPA both in vivo and in vitro. However, Karbownik et al. cannot exclude a direct pro-oxidative effect of IPA, which was suggested because of alterations in membrane fluidity after IPA treatment.

An objective of this project was to identify hepatoprotective effects of IPA. Therefore cultured primary hepatocytes were used because they represent a system considered biochemically equivalent to an intact liver for haloalkane effects and are, as suggested by Soars et al., more useful than hepatic microsomes in terms of accomplishing a better in vitro – in vivo extrapolation.<sup>32,65,66</sup>

In a systematic approach, the conscientious establishment of standard operating procedures and commitment to them (e.g., for hepatocyte isolation, growing

cultures, and modeling cytotoxicity) was deemed crucial to obtaining reproducible results.

Preparatory steps were strictly standardized. As the literature suggested for hepatocyte isolation, the viability of primary hepatocytes depends on factors such as perfusate flow and complete solubility of the reagents. Cannulation of the VCI and retrograde perfusion was favored because of the reproducibility of the same viability and easier cannulation compared to perfusion via the portal vein.<sup>30</sup>

Dedifferentiation of the hepatocytes in vitro was anticipated and so as a precautionary measure, the experimental design was adapted to ensure validity of the model.<sup>67</sup> Subsequently, a short period of culturing and serum starvation of the hepatocytes was favored (hepatocytes were harvested 26h after seeding).<sup>68</sup> Other factors such as the extracellular environment of cultured hepatocytes and media supplements were considered after consulting the latest literature. Concerning the extracellular matrix and its configuration, Tuschl et al. conclude from their protein profiling studies on cultured primary murine hepatocytes that collagen-monolayer-culture conditions in serum-free media maintains liver-like features for the required time period and was therefore validated as appropriate to the study design. Nevertheless, 3D spherical organoids are used because they replicate the in vivo functions of the liver better than the hepatocyte monolayer culture does.<sup>69,70</sup>

The CCl<sub>4</sub> cytotoxicity model chosen in this study is well established as an excellent tool in the liver research community.<sup>32</sup> Hepatic injury induced through CCl<sub>4</sub> has been used extensively in experimental models to understand and evaluate the therapeutic potential of dietary antioxidants and drugs.<sup>71</sup>

In his review, Weber et al. analyzed CCl<sub>4</sub> as a toxicological model and describes CCl<sub>4</sub> as an important model substance for studying hepatotoxic effects such as fatty degeneration, hepatocellular death, carcinogenicity, and fibrosis. He outlines that CCl<sub>4</sub> toxicity depends on dose, exposure time, the presence of potentiating agents, and on the age of the affected organism. In a finely tuned balance, the CCl<sub>4</sub> model reveals the opportunity in vivo for full regeneration from liver damage.

One major drawback of this model, from a practical point of view, is the volatility of CCl<sub>4</sub>.<sup>32</sup>

Clawson et al. conclude that hypomethylation of ribosomal RNA takes place in CCl<sub>4</sub>-mediated cellular damage and parallels the CCl<sub>4</sub>-induced inhibition of protein synthesis, which could affect the protein expression level analysis in this study.<sup>72,73</sup>

Furthermore, FCS in the culture medium was found to interfere with the CCl<sub>4</sub>-induced toxicity over a time period of 24h. The literature suggests a significant amount of SOD activity in the FCS, which is considered to be a possible explanation for the observed results.<sup>74</sup>

Central to CCl<sub>4</sub> toxicity are the cytochromes P450 (CYPs), and subsequently CYP2E1 knockout mice were resistant to hepatotoxicity induced by CCl<sub>4</sub>.<sup>54</sup> CYP2E1 activates CCl<sub>4</sub> and the trichloromethyl CCl<sub>3</sub><sup>\*</sup> is formed.

Because all hepatotoxic effects originate in the bioactivation of CYP2E1, its concentration was monitored precisely.

Considering the results presented in section 4.3.2, no significant changes in CYP2E1 levels compared to the control condition were found. Equal bioactivation of CCl<sub>4</sub> and, subsequently, equal hepatotoxic effect in all experiments can be assumed. However, in CCl<sub>4</sub>-treated cultures, the mean CYP2E1 protein level is likely to be lower than the control according to the literature. In line with this consideration, a 4-fold decrease of CYP2E1 could be valued within the CCl<sub>4</sub> condition.<sup>75</sup>

The immunodetectable protein contents of CYP2E1 are known to be downregulated time-dependently after CCl<sub>4</sub> treatment. This is probably due to specific destruction caused by its own metabolized substrate.<sup>76</sup> CYP2E1 was also reported to have a very short half-life of 7-8h, suggesting a susceptibility to proteolysis. This would explain the observed trend reported in section 4.3.2.<sup>77</sup>

One of the most important findings of this study, enzyme leakage of the intracellular enzymes LDH and ALT was significantly reduced by IPA in a dose-dependent manner in primary hepatocytes. All measured results were in the linearity-range of the test setup (compare section 3.4.3.1). It is therefore evident

that a correlation between IPA concentration and hepatoprotection in vitro exists.

These results are in agreement with those obtained by prior studies.

Chyan et al. assume from three independent duplicate experiments with SK-N-SH human neuroblastoma cells exposed to the superoxide dismutase inhibitor diethyldithiocarbamate (DDTC) or to oxidative stress mediated by  $H_2O_2$ , a neuroprotective effect, using Trypan Blue exclusion. In their analysis, Chyan et al. quantify a protective effect of IPA in neurons, which they show to be at least twice as potent as the antioxidant melatonin and exceeds the melatonin serum concentration in vivo. By applying an IPA concentration up to  $100\mu M$ , the maximum protective effect, which more precisely suggests a saturation value, was reached with  $10\mu M$ .

Lefler et al. conducted experiments in vivo of IPA pretreatment ( $10\text{mg/kg}$ ) in mice prior to an ischemic event, modeling liver transplantation. Their focus was on the prevention of excessive tissue damage and so liver enzymes were used as markers for liver dysfunction. A significant decrease of both ALT and AST were found in a 2h reperfusion period.<sup>78</sup>

The aforementioned mechanisms of  $CCl_4$  toxicity provoke cell damage, reflected by structural changes and membrane disintegration. Concomitantly to enzyme release, dye uptake of Propidium Iodide increased after  $CCl_4$  treatment and necrotic structural changes were seen microscopically, which facilitated the estimation of the extent of cell damage.

The detailed mechanism of  $CCl_4$  hepatotoxic effects on a molecular level is mediated via  $CCl_3^{\cdot}$ <sup>79</sup> and its derivatives binding to cellular molecules as proteins, nucleic acids, and lipids.

The highly reactive radicals are known to impair essential metabolic processes such as lipid metabolism. They also affect DNA as they form adducts between the nucleic acids, and in the presence of oxygen, they launch the chain reaction of lipid peroxidation.<sup>79</sup>

The trichloromethyl peroxy radical ( $CCl_3OO^{\cdot}$ ) is mainly responsible for lipid peroxidation<sup>80</sup>, which affects polyunsaturated fatty acids (PUFA), particularly

those related to phospholipids. As a result of lipid peroxidation, fluidity and permeability of the plasma membrane, of the mitochondrial membranes, and of the endoplasmic reticulum's membrane are changed pathologically.

Subsequently, the calcium homeostasis and sequestration among other things are affected and contribute to total cellular damage.<sup>81</sup>

The most important mechanism of CCl<sub>4</sub>-induced toxicity, haloalkylation or lipid peroxidation, contributes the most to radically induced cell damage and cell necrosis in hepatocytes and is discussed herein.

This study focused on the TBARS assay to measure the aldehydic secondary products of lipid peroxidation as Malondialdehyde (MDA) and 4-hydroxynonenal (4-HNE).

The current study found a significant induction of lipid peroxidation due to CCl<sub>4</sub> and a dose-dependent reduction of TBARS after IPA treatment. Again, dose-dependency strongly suggests a hepatoprotective effect of IPA.

These results are further supported by the findings of Karbownik et al., who experimentally induced oxidative changes in rat hepatic microsomal membranes with FeCl<sub>3</sub> (0.2 mM), ADP (1.7 mM) and NADPH (0.2 mM) and found a decrease of lipid peroxidation with a ten times higher IPA concentration as compared to the results in this study. This might be due to the forceful lipid peroxidation potential of ADP-Fe<sup>3+</sup>, which is five to six times that of CCl<sub>4</sub>.<sup>82</sup>

Poeggeler et al. found IPA directly scavenging hydroxyl radicals with a rate constant of  $7.8 \times 10^{10} \text{ mol l}^{-1} \text{ s}^{-1}$ . They also found that IPA attenuated the hydrogen peroxide-induced, hydroxyl radical-mediated MDA formation in rat striatal homogenates in a concentration-dependent manner with 50% of inhibition mediated by 180  $\mu\text{M}$  of IPA. Interestingly, IPA's hydroxyl radical-scavenging efficacy was potentiated with co-treatment of the endogenous antioxidant glutathione, suggesting that there might be a symbiotic relationship between the bacteria-derived products and the cellular homeostasis.

SOD1 is a copper and zinc-containing homodimer and is found in cytoplasm, nucleus, microsomes, and in the intermembrane space of mitochondria.<sup>83,84</sup>

Miao et al. found as transcriptional factors of the SOD enzyme family NF- $\kappa$ B, Sp1, AP-1, AP-2, and CCAAT-enhancer-binding protein (C/EBP).

Venkatesh et al. conjecture that a cellular target of IPA exists but is not evident in the recent literature. To ascertain if IPA could potentially regulate intestinal barrier function through the nuclear pregnane X receptor (PXR), in vitro and in vivo studies of the effect of IPA on inflammation and gut barrier function were conducted, and the regulatory function of IPA in enteric inflammation through the PXR could be demonstrated.

IPA was identified as a ligand for PXR in vivo and further downregulated TNF- $\alpha$  while it upregulated junctional protein-coding mRNAs in enterocytes.<sup>15</sup>

In this study, SOD1 protein concentration was found to be upregulated significantly when hepatocytes were stressed with CCl<sub>4</sub> in co-incubation with 1 $\mu$ M IPA. A tendency of SOD1 protein induction under solely IPA treatment was even significant for 0.1 $\mu$ M IPA compared to the baseline of the control. A possible explanation for these results might be that an intracellular signal transduction in hepatocytes with a subsequent enzyme induction, as was recently found in enterocytes, exists. As the hepatocytes culture was serum starved during the IPA incubation, low basal activities of hepatocytes but high responsiveness to specific stimuli was assured according to Klingmüller et al., and cells were generally susceptible to small changes in ligand concentration of intracellular signal transduction. Therefore an upregulation of SOD1 could be the result of an unknown IPA ligand function. These findings could help expand the present antioxidant role of IPA. To develop a full picture of IPA's role in hepatocytes, additional studies to investigate the dynamics of protein induction with more powerful methods than solely protein expression levels are needed. ROS are released in the liver as physiological inflammatory response by resident macrophages (Kupffer cells) or by activated and recruited monocytes or neutrophils.<sup>85,86</sup> ROS-induced intracellular oxidant stress in hepatocytes involves the promotion of mitochondrial dysfunction and contributes primarily to oncotic necrosis and less apoptosis.<sup>86</sup> While effects that influence the cell directly were depicted within this type of in vitro model, the significant role of non-parenchymal



cells and the inflammatory response of the liver tissue to CCl<sub>4</sub> treatment of hepatocytes, as mediated by proinflammatory cytokines such as TNF- $\alpha$  and released ROS, were beyond the scope of this study.<sup>35,87</sup>

HSP27 is a protein that exhibits chaperone-like activity. It is induced by diverse mechanisms and is currently understood to play an ambiguous role with cytoprotective (chaperone-like activity, anti-apoptotic) as well as partly oncogenic<sup>64</sup> properties.

In this study, HSP27 was significantly reduced under CCl<sub>4</sub> treatment. By contrast, HSP70 protein increased by 20% after 24h of CCl<sub>4</sub> treatment in vivo (Knockaert et al.<sup>88</sup>).

An important finding was the significant upregulation of HSP27 after co-incubation with IPA and CCl<sub>4</sub> compared to both the control and to the CCl<sub>4</sub> treatment.

## 6 Bibliography

- 1 Juza, R. M. & Pauli, E. M. Clinical and surgical anatomy of the liver: a review for clinicians. *Clin Anat* **27**, 764-769, doi:10.1002/ca.22350 (2014).
- 2 Kmiec, Z. Cooperation of liver cells in health and disease. *Advances in anatomy, embryology, and cell biology* **161**, III-XIII, 1-151 (2001).
- 3 Seki, E. & Schnabl, B. Role of innate immunity and the microbiota in liver fibrosis: crosstalk between the liver and gut. *The Journal of physiology* **590**, 447-458, doi:10.1113/jphysiol.2011.219691 (2012).
- 4 Yan, A. W. *et al.* Enteric dysbiosis associated with a mouse model of alcoholic liver disease. *Hepatology* **53**, 96-105, doi:10.1002/hep.24018 (2011).
- 5 Fouts, D. E., Torralba, M., Nelson, K. E., Brenner, D. A. & Schnabl, B. Bacterial translocation and changes in the intestinal microbiome in mouse models of liver disease. *Journal of hepatology*, doi:10.1016/j.jhep.2012.01.019 (2012).
- 6 Szabo, G. Gut-liver axis in alcoholic liver disease. *Gastroenterology* **148**, 30-36, doi:10.1053/j.gastro.2014.10.042 (2015).
- 7 Brenner, D. A. *et al.* Non-alcoholic steatohepatitis-induced fibrosis: Toll-like receptors, reactive oxygen species and Jun N-terminal kinase. *Hepatology research : the official journal of the Japan Society of Hepatology* **41**, 683-686, doi:10.1111/j.1872-034X.2011.00814.x (2011).
- 8 Miura, K. *et al.* Toll-like receptor 9 promotes steatohepatitis by induction of interleukin-1beta in mice. *Gastroenterology* **139**, 323-334 e327, doi:10.1053/j.gastro.2010.03.052 (2010).
- 9 Schnabl, B. *et al.* A TLR4/MD2 fusion protein inhibits LPS-induced pro-inflammatory signaling in hepatic stellate cells. *Biochemical and biophysical research communications* **375**, 210-214, doi:10.1016/j.bbrc.2008.07.150 (2008).
- 10 Benten, D. & Wiest, R. Gut microbiome and intestinal barrier failure--the "Achilles heel" in hepatology? *Journal of hepatology* **56**, 1221-1223, doi:10.1016/j.jhep.2012.03.003 (2012).
- 11 Mazagova, M. *et al.* Commensal microbiota is hepatoprotective and prevents liver fibrosis in mice. *FASEB journal : official publication of the Federation of American Societies for Experimental Biology*, doi:10.1096/fj.14-259515 (2014).
- 12 Wikoff, W. R. *et al.* Metabolomics analysis reveals large effects of gut microflora on mammalian blood metabolites. *Proceedings of the National Academy of Sciences of the United States of America* **106**, 3698-3703, doi:10.1073/pnas.0812874106 (2009).
- 13 Elsdon, S. R., Hilton, M. G. & Waller, J. M. The end products of the metabolism of aromatic amino acids by Clostridia. *Archives of microbiology* **107**, 283-288 (1976).

- 14 Young, S. N., Anderson, G. M., Gauthier, S. & Purdy, W. C. The origin of indoleacetic acid and indolepropionic acid in rat and human cerebrospinal fluid. *Journal of neurochemistry* **34**, 1087-1092 (1980).
- 15 Venkatesh, M. *et al.* Symbiotic bacterial metabolites regulate gastrointestinal barrier function via the xenobiotic sensor PXR and Toll-like receptor 4. *Immunity* **41**, 296-310, doi:10.1016/j.immuni.2014.06.014 (2014).
- 16 Bansal, T., Alaniz, R. C., Wood, T. K. & Jayaraman, A. The bacterial signal indole increases epithelial-cell tight-junction resistance and attenuates indicators of inflammation. *Proceedings of the National Academy of Sciences of the United States of America* **107**, 228-233, doi:10.1073/pnas.0906112107 (2010).
- 17 Wu, S., Yi, J., Zhang, Y. G., Zhou, J. & Sun, J. Leaky intestine and impaired microbiome in an amyotrophic lateral sclerosis mouse model. *Physiological reports* **3**, doi:10.14814/phy2.12356 (2015).
- 18 Indo, H. P. *et al.* A mitochondrial superoxide theory for oxidative stress diseases and aging. *Journal of clinical biochemistry and nutrition* **56**, 1-7, doi:10.3164/jcbrn.14-42 (2015).
- 19 Chyan, Y. J. *et al.* Potent neuroprotective properties against the Alzheimer beta-amyloid by an endogenous melatonin-related indole structure, indole-3-propionic acid. *The Journal of biological chemistry* **274**, 21937-21942 (1999).
- 20 Karbownik, M. *et al.* Indole-3-propionic acid, a melatonin-related molecule, protects hepatic microsomal membranes from iron-induced oxidative damage: relevance to cancer reduction. *Journal of cellular biochemistry* **81**, 507-513 (2001).
- 21 Wyllie, A. H., Kerr, J. F. & Currie, A. R. Cell death: the significance of apoptosis. *International review of cytology* **68**, 251-306 (1980).
- 22 Saraste, A. Morphologic criteria and detection of apoptosis. *Herz* **24**, 189-195 (1999).
- 23 Crompton, T., Peitsch, M. C., MacDonald, H. R. & Tschopp, J. Propidium iodide staining correlates with the extent of DNA degradation in isolated nuclei. *Biochemical and biophysical research communications* **183**, 532-537 (1992).
- 24 Nicoletti, I., Migliorati, G., Pagliacci, M. C., Grignani, F. & Riccardi, C. A rapid and simple method for measuring thymocyte apoptosis by propidium iodide staining and flow cytometry. *Journal of immunological methods* **139**, 271-279 (1991).
- 25 Groneberg, D. A., Grosse-Siestrup, C. & Fischer, A. In vitro models to study hepatotoxicity. *Toxicologic pathology* **30**, 394-399 (2002).
- 26 Boess, F. *et al.* Gene expression in two hepatic cell lines, cultured primary hepatocytes, and liver slices compared to the in vivo liver gene expression in rats: possible implications for toxicogenomics use of in vitro systems. *Toxicological sciences : an official journal of the Society of Toxicology* **73**, 386-402, doi:10.1093/toxsci/kfg064 (2003).
- 27 Berry, M. N. & Friend, D. S. High-yield preparation of isolated rat liver parenchymal cells: a biochemical and fine structural study. *The Journal of cell biology* **43**, 506-520 (1969).

- 28 Shen, L., Hillebrand, A., Wang, D. Q. & Liu, M. Isolation and primary culture of rat hepatic cells. *Journal of visualized experiments : JoVE*, doi:10.3791/3917 (2012).
- 29 Goncalves, L. A., Vigario, A. M. & Penha-Goncalves, C. Improved isolation of murine hepatocytes for in vitro malaria liver stage studies. *Malaria journal* **6**, 169, doi:10.1186/1475-2875-6-169 (2007).
- 30 Casciano, D. A. Development and utilization of primary hepatocyte culture systems to evaluate metabolism, DNA binding, and DNA repair of xenobiotics. *Drug metabolism reviews* **32**, 1-13, doi:10.1081/DMR-100100561 (2000).
- 31 Ulrich, R. G. *et al.* Cultured hepatocytes as investigational models for hepatic toxicity: practical applications in drug discovery and development. *Toxicology letters* **82-83**, 107-115 (1995).
- 32 Weber, L. W., Boll, M. & Stampfl, A. Hepatotoxicity and mechanism of action of haloalkanes: carbon tetrachloride as a toxicological model. *Critical reviews in toxicology* **33**, 105-136, doi:10.1080/713611034 (2003).
- 33 Liu, Y. J. *et al.* Anti-inflammatory and hepatoprotective effects of Ganoderma lucidum polysaccharides on carbon tetrachloride-induced hepatocyte damage in common carp (*Cyprinus carpio* L.). *International immunopharmacology* **25**, 112-120, doi:10.1016/j.intimp.2015.01.023 (2015).
- 34 Taniguchi, M., Takeuchi, T., Nakatsuka, R., Watanabe, T. & Sato, K. Molecular process in acute liver injury and regeneration induced by carbon tetrachloride. *Life sciences* **75**, 1539-1549, doi:10.1016/j.lfs.2004.02.030 (2004).
- 35 Luster, M. I. *et al.* Role of inflammation in chemical-induced hepatotoxicity. *Toxicology letters* **120**, 317-321 (2001).
- 36 Amacher, D. E., Fasulo, L. M., Charuel, C., Comby, P. & Beaumont, K. In vitro toxicity of zamifenacin (UK-76,654) and metabolites in primary hepatocyte cultures. *Xenobiotica; the fate of foreign compounds in biological systems* **28**, 895-908, doi:10.1080/004982598239137 (1998).
- 37 Bergmeyer, H. U., Horder, M. & Rej, R. International Federation of Clinical Chemistry (IFCC) Scientific Committee, Analytical Section: approved recommendation (1985) on IFCC methods for the measurement of catalytic concentration of enzymes. Part 3. IFCC method for alanine aminotransferase (L-alanine: 2-oxoglutarate aminotransferase, EC 2.6.1.2). *Journal of clinical chemistry and clinical biochemistry. Zeitschrift fur klinische Chemie und klinische Biochemie* **24**, 481-495 (1986).
- 38 Nakae, Y. & Stoward, P. J. Kinetic parameters of lactate dehydrogenase in liver and gastrocnemius determined by three quantitative histochemical methods. *The journal of histochemistry and cytochemistry : official journal of the Histochemistry Society* **45**, 1427-1431 (1997).
- 39 Renart, J., Reiser, J. & Stark, G. R. Transfer of proteins from gels to diazobenzyloxymethyl-paper and detection with antisera: a method for studying antibody specificity and antigen structure. *Proceedings of the National Academy of Sciences of the United States of America* **76**, 3116-3120 (1979).

- 40 Towbin, H., Staehelin, T. & Gordon, J. Electrophoretic transfer of proteins from polyacrylamide gels to nitrocellulose sheets: procedure and some applications. *Proceedings of the National Academy of Sciences of the United States of America* **76**, 4350-4354 (1979).
- 41 Aebersold, R. H., Leavitt, J., Saavedra, R. A., Hood, L. E. & Kent, S. B. Internal amino acid sequence analysis of proteins separated by one- or two-dimensional gel electrophoresis after in situ protease digestion on nitrocellulose. *Proceedings of the National Academy of Sciences of the United States of America* **84**, 6970-6974 (1987).
- 42 Walker, J. M. The bicinchoninic acid (BCA) assay for protein quantitation. *Methods Mol Biol* **32**, 5-8, doi:10.1385/0-89603-268-X:5 (1994).
- 43 Noble, J. E. & Bailey, M. J. Quantitation of protein. *Methods in enzymology* **463**, 73-95, doi:10.1016/S0076-6879(09)63008-1 (2009).
- 44 Brenner, A. J. & Harris, E. D. A quantitative test for copper using bicinchoninic acid. *Analytical biochemistry* **226**, 80-84, doi:10.1006/abio.1995.1194 (1995).
- 45 Jacobson, G. & Karsnas, P. Important parameters in semi-dry electrophoretic transfer. *Electrophoresis* **11**, 46-52, doi:10.1002/elps.1150110111 (1990).
- 46 Aoyama, T. *et al.* Nicotinamide adenine dinucleotide phosphate oxidase in experimental liver fibrosis: GKT137831 as a novel potential therapeutic agent. *Hepatology* **56**, 2316-2327, doi:10.1002/hep.25938 (2012).
- 47 Taylor, S. C., Berkelman, T., Yadav, G. & Hammond, M. A defined methodology for reliable quantification of Western blot data. *Molecular biotechnology* **55**, 217-226, doi:10.1007/s12033-013-9672-6 (2013).
- 48 Ramey, G., Deschemin, J. C. & Vaulont, S. Cross-talk between the mitogen activated protein kinase and bone morphogenetic protein/hemojuvelin pathways is required for the induction of hepcidin by holotransferrin in primary mouse hepatocytes. *Haematologica* **94**, 765-772, doi:10.3324/haematol.2008.003541 (2009).
- 49 Chirdchupunseree, H. & Pramyothin, P. Protective activity of phyllanthin in ethanol-treated primary culture of rat hepatocytes. *Journal of ethnopharmacology* **128**, 172-176, doi:10.1016/j.jep.2010.01.003 (2010).
- 50 Vinken, M. *et al.* Characterization of spontaneous cell death in monolayer cultures of primary hepatocytes. *Archives of toxicology* **85**, 1589-1596, doi:10.1007/s00204-011-0703-4 (2011).
- 51 Muller, A. S. & Pallauf, J. Effect of increasing selenite concentrations, vitamin E supplementation and different fetal calf serum content on GPx1 activity in primary cultured rabbit hepatocytes. *J Trace Elem Med Biol* **17**, 183-192 (2003).
- 52 Berry, M. N., Grivell, A. R., Grivell, M. B. & Phillips, J. W. Isolated hepatocytes--past, present and future. *Cell biology and toxicology* **13**, 223-233 (1997).
- 53 Yu, C. *et al.* Increased carbon tetrachloride-induced liver injury and fibrosis in FGFR4-deficient mice. *The American journal of pathology* **161**, 2003-2010, doi:10.1016/S0002-9440(10)64478-1 (2002).
- 54 Wong, F. W., Chan, W. Y. & Lee, S. S. Resistance to carbon tetrachloride-induced hepatotoxicity in mice which lack CYP2E1 expression. *Toxicology*

- and applied pharmacology* **153**, 109-118, doi:10.1006/taap.1998.8547 (1998).
- 55 Cheeseman, K. H., Albano, E. F., Tomasi, A. & Slater, T. F. Biochemical studies on the metabolic activation of halogenated alkanes. *Environmental health perspectives* **64**, 85-101 (1985).
- 56 Schulz, R. *et al.* Inhibiting the HSP90 chaperone destabilizes macrophage migration inhibitory factor and thereby inhibits breast tumor progression. *The Journal of experimental medicine* **209**, 275-289, doi:10.1084/jem.20111117 (2012).
- 57 Pal, A. *et al.* The sigma-1 receptor protects against cellular oxidative stress and activates antioxidant response elements. *European journal of pharmacology* **682**, 12-20, doi:10.1016/j.ejphar.2012.01.030 (2012).
- 58 Sakurai, T. *et al.* Hepatocyte necrosis induced by oxidative stress and IL-1 alpha release mediate carcinogen-induced compensatory proliferation and liver tumorigenesis. *Cancer cell* **14**, 156-165, doi:10.1016/j.ccr.2008.06.016 (2008).
- 59 Kaur, S. J., McKeown, S. R. & Rashid, S. Mutant SOD1 mediated pathogenesis of Amyotrophic Lateral Sclerosis. *Gene* **577**, 109-118, doi:10.1016/j.gene.2015.11.049 (2016).
- 60 Spalloni, A. & Longone, P. Cognitive impairment in amyotrophic lateral sclerosis, clues from the SOD1 mouse. *Neuroscience and biobehavioral reviews* **60**, 12-25, doi:10.1016/j.neubiorev.2015.11.006 (2016).
- 61 Che, M., Wang, R., Li, X., Wang, H. Y. & Zheng, X. F. Expanding roles of superoxide dismutases in cell regulation and cancer. *Drug discovery today* **21**, 143-149, doi:10.1016/j.drudis.2015.10.001 (2016).
- 62 Fukai, T. & Ushio-Fukai, M. Superoxide dismutases: role in redox signaling, vascular function, and diseases. *Antioxidants & redox signaling* **15**, 1583-1606, doi:10.1089/ars.2011.3999 (2011).
- 63 Bakthisaran, R., Tangirala, R. & Rao, C. M. Small heat shock proteins: Role in cellular functions and pathology. *Biochimica et biophysica acta* **1854**, 291-319, doi:10.1016/j.bbapap.2014.12.019 (2014).
- 64 Garrido, C. *et al.* Heat shock proteins 27 and 70: anti-apoptotic proteins with tumorigenic properties. *Cell Cycle* **5**, 2592-2601 (2006).
- 65 Soars, M. G., McGinnity, D. F., Grime, K. & Riley, R. J. The pivotal role of hepatocytes in drug discovery. *Chemico-biological interactions* **168**, 2-15, doi:10.1016/j.cbi.2006.11.002 (2007).
- 66 Wang, K., Shindoh, H., Inoue, T. & Horii, I. Advantages of in vitro cytotoxicity testing by using primary rat hepatocytes in comparison with established cell lines. *The Journal of toxicological sciences* **27**, 229-237 (2002).
- 67 Elaut, G. *et al.* Molecular mechanisms underlying the dedifferentiation process of isolated hepatocytes and their cultures. *Current drug metabolism* **7**, 629-660 (2006).
- 68 Clayton, D. F. & Darnell, J. E., Jr. Changes in liver-specific compared to common gene transcription during primary culture of mouse hepatocytes. *Molecular and cellular biology* **3**, 1552-1561 (1983).

- 69 Mingoia, R. T., Nabb, D. L., Yang, C. H. & Han, X. Primary culture of rat hepatocytes in 96-well plates: effects of extracellular matrix configuration on cytochrome P450 enzyme activity and inducibility, and its application in in vitro cytotoxicity screening. *Toxicology in vitro : an international journal published in association with BIBRA* **21**, 165-173, doi:10.1016/j.tiv.2006.10.012 (2007).
- 70 Lu, Y. *et al.* A novel 3D liver organoid system for elucidation of hepatic glucose metabolism. *Biotechnology and bioengineering* **109**, 595-604, doi:10.1002/bit.23349 (2012).
- 71 Basu, S. Carbon tetrachloride-induced lipid peroxidation: eicosanoid formation and their regulation by antioxidant nutrients. *Toxicology* **189**, 113-127 (2003).
- 72 Clawson, G. A., MacDonald, J. R. & Woo, C. H. Early hypomethylation of 2'-O-ribose moieties in hepatocyte cytoplasmic ribosomal RNA underlies the protein synthetic defect produced by CCl<sub>4</sub>. *The Journal of cell biology* **105**, 705-711 (1987).
- 73 Smuckler, E. A. & Benditt, E. P. Studies on Carbon Tetrachloride Intoxication. 3. A Subcellular Defect in Protein Synthesis. *Biochemistry* **4**, 671-679 (1965).
- 74 Baret, A. & Emerit, I. Variation of superoxide dismutase levels in fetal calf serum. *Mutation research* **121**, 293-297 (1983).
- 75 Guzelian, P. S. & Swisher, R. W. Degradation of cytochrome P-450 haem by carbon tetrachloride and 2-allyl-2-isopropylacetamide in rat liver in vivo and in vitro. Involvement of non-carbon monoxide-forming mechanisms. *The Biochemical journal* **184**, 481-489 (1979).
- 76 Sohn, D. H., Yun, Y. P., Park, K. S., Veech, R. L. & Song, B. J. Post-translational reduction of cytochrome P450IIE by CCl<sub>4</sub>, its substrate. *Biochemical and biophysical research communications* **179**, 449-454 (1991).
- 77 Tierney, D. J., Haas, A. L. & Koop, D. R. Degradation of cytochrome P450 2E1: selective loss after labilization of the enzyme. *Archives of biochemistry and biophysics* **293**, 9-16 (1992).
- 78 Lefler, S. R. *et al.* Amelioration of hepatic ischemia/reperfusion injury using indolepropionic acid. *Transplantation proceedings* **34**, 3065-3066 (2002).
- 79 McCay, P. B., Lai, E. K., Poyer, J. L., DuBose, C. M. & Janzen, E. G. Oxygen- and carbon-centered free radical formation during carbon tetrachloride metabolism. Observation of lipid radicals in vivo and in vitro. *The Journal of biological chemistry* **259**, 2135-2143 (1984).
- 80 Mico, B. A. & Pohl, L. R. Reductive oxygenation of carbon tetrachloride: trichloromethylperoxyl radical as a possible intermediate in the conversion of carbon tetrachloride to electrophilic chlorine. *Archives of biochemistry and biophysics* **225**, 596-609 (1983).
- 81 Harman, A. W. & Maxwell, M. J. An evaluation of the role of calcium in cell injury. *Annual review of pharmacology and toxicology* **35**, 129-144, doi:10.1146/annurev.pa.35.040195.001021 (1995).
- 82 Boll, M., Weber, L. W., Becker, E. & Stampfl, A. Mechanism of carbon tetrachloride-induced hepatotoxicity. Hepatocellular damage by reactive

- carbon tetrachloride metabolites. *Zeitschrift fur Naturforschung. C, Journal of biosciences* **56**, 649-659 (2001).
- 83 Miao, L. & St Clair, D. K. Regulation of superoxide dismutase genes: implications in disease. *Free radical biology & medicine* **47**, 344-356, doi:10.1016/j.freeradbiomed.2009.05.018 (2009).
- 84 Zelko, I. N., Mariani, T. J. & Folz, R. J. Superoxide dismutase multigene family: a comparison of the CuZn-SOD (SOD1), Mn-SOD (SOD2), and EC-SOD (SOD3) gene structures, evolution, and expression. *Free radical biology & medicine* **33**, 337-349 (2002).
- 85 Kamata, H. *et al.* Reactive oxygen species promote TNFalpha-induced death and sustained JNK activation by inhibiting MAP kinase phosphatases. *Cell* **120**, 649-661, doi:10.1016/j.cell.2004.12.041 (2005).
- 86 Jaeschke, H. Reactive oxygen and mechanisms of inflammatory liver injury: Present concepts. *Journal of gastroenterology and hepatology* **26 Suppl 1**, 173-179, doi:10.1111/j.1440-1746.2010.06592.x (2011).
- 87 Luster, M. I. *et al.* The role of tumor necrosis factor alpha in chemical-induced hepatotoxicity. *Annals of the New York Academy of Sciences* **919**, 214-220 (2000).
- 88 Knockaert, L. *et al.* Carbon tetrachloride-mediated lipid peroxidation induces early mitochondrial alterations in mouse liver. *Laboratory investigation; a journal of technical methods and pathology* **92**, 396-410, doi:10.1038/labinvest.2011.193 (2012).



## 7 Acknowledgments

I wish to express my sincere thanks to Bernd Schnabl, David Brenner, and Prof. Dr. med. Claus Hellerbrand for providing me with all the necessary facilities for the research and for their personal advice. I would also like to thank my parents for all their wise counsel and sympathetic ear. You are always there for me.

Max Wißmüller

Regensburg, October 21st, 2016

## 8 Curriculum Vitae

### Persönliche Daten

---

Name	Max Vincenz Jan Wißmüller
Geburtsdatum	13.6.1987
Geburtsort	Sulzbach-Rosenberg
Familienstand	ledig
Eltern	Karl-Theodor Wißmüller, Dipl. Pädagoge, Diakonisches Werk Sulzbach Teresa Wißmüller, geb. Falsett Dipl. Soziologin, Sozialpsychiatrisches Zentrum Amberg
Geschwister	Elisabeth, *1984 Niklas, *1989

### Ausbildung

---

Okt. 2007- Okt. 2014:	<b>Universität Regensburg, Studium der Humanmedizin</b> Ärztliche Prüfung: Gesamtnote „gut“ (2,33)
Sept. 1996- Juni 2006:	<b>Herzog- Christian- August Gymnasium Sulzbach</b> Leistungskurse: Geschichte, Sozialkunde und Mathematik Allgemeine Hochschulreife: 1,3

### Berufserfahrung

---

Juli 2015- Sept. 2016	<b>Assistenzarzt für Neurologie an der Universitätsklinik Basel</b> (Prof. Dr. med. Ludwig Kappos)
März 2013-Jan. 2014	<b>1. PJ- Tertian Innere Medizin, Kantonspital Chur, Schweiz</b> (Prof. Dr. med. Walter Reinhart)  <b>2. PJ- Tertian Chirurgie, KH Barmherzige Brüder, Regensburg</b> Abteilungen: Visceralchirurgie (Prof. Dr. med. Piso); Orthopädie (Prof. Dr. med. Füchtmeier), Thoraxchirurgie (Prof. Dr. med. Hofmann)  <b>3. PJ-Tertian Neurologie, Neurologische Universitätsklinik, Regensburg</b> (Prof. Dr. med. Ulrich Bogdahn)
März 2012	<b>VA Medical Center, San Diego, USA</b> Famulatur in der Division of Gastroenterology
März 2011	<b>Charité Campus Mitte, Berlin</b>

Famulatur in der Intensivmedizin

März 2010

**St. Georg Krankenhaus, Hamburg**  
Famulatur in der Unfallchirurgie

Aug. 2006 – April 2007

**Zivildienst am St. Anna Krankenhaus, Sulzbach-Rosenberg**  
Stationäre Patientenversorgung

## **Publikationen**

---

Mazagova, M.; Wang, L.; Anfora, A. T.; **Wissmueller, M.**; Lesley, S. A.; Miyamoto, Y.; Eckmann, L.; Dhungana, S.; Pathmasiri, W.; Sumner, S.; Westwater, C.; Brenner, D. A.; Schnabl, B. Commensal microbiota is hepatoprotective and prevents liver fibrosis in mice. *FASEB journal : official publication of the Federation of American Societies for Experimental Biology*, doi:10.1096/fj.14-259515 (2014).

## **Aktivitäten außerhalb des Curriculums**

---

Nov. 2014 – Juni 2015

**Heinz Nixdorf Stiftung**, Herausforderung Unternehmertum

Sept. 2011- Feb. 2012

**University of California San Diego, Forschungsaufenthalt**  
Arbeitsgruppe MD Dr. David Brenner, *Vice-Chancellor* der UCSD

Juni 2011 –Juni 2014

**Stipendiat der Stiftung der Deutschen Wirtschaft**

Mai 2010-Juli 2011

**Universität Regensburg, Stammzellforschung**  
Arbeitsgruppe Dr. Grassinger, Hämatologie/Onkologie

Juli 2010- Juli 2011

**Universitätsklinik Regensburg, Abteilung für Unfallchirurgie**  
Wissenschaftliche Hilfskraft in der Verkehrsunfallforschung

Okt. 2008- März 2009

**Universität Regensburg**  
Wissenschaftliche Hilfskraft am Institut für Anatomie

Interessen

Bergwandern, Triathlon, Literatur, Kabarett, Musik

## **Ehrenamt/Zusatzqualifikationen**

---

Sprachen

Englisch, verhandlungssicher  
Spanisch, Grundkenntnisse

Soziales Engagement

Migrantenmedizin Regensburg e.V.; Bahnhofsmision;  
Familientreff e.V.; Schülersprecher